environmental microbiology

Environmental Microbiology (2021) **23**(4), 2293–2314 doi:10.1111/1462-2920.15416

# The infection cushion of *Botrytis cinerea*: a fungal 'weapon' of plant-biomass destruction

**Mathias Choquer [1,2*†] Christine Rascle,[1,2] Isabelle R. Gonçalves,[1,2] Amélie de Vallée,[1,2] Cécile Ribot,[1] Elise Loisel,[1,2] Pavlé Smilevski,[1,2] Jordan Ferria,[1,2] Mahamadi Savadogo,[1,2] Eytham Souibgui,[1,2] Marie-Josèphe Gagey,[1,2] Jean-William Dupuy [3] Jeffrey A. Rollins,[4] Riccardo Marcato,[2,5] Camille Noûs,[1] Christophe Bruel [1,2†] and Nathalie Poussereau [1,2†]**

[1]*Univ Lyon, Université Lyon 1, CNRS, INSA-Lyon, Microbiologie, Adaptation et Pathogénie, UMR 5240 MAP, 10 Rue Raphaël Dubois, Villeurbanne, F-69622, France.*

[2]*Bayer SAS, Crop Science Division, Laboratoire Mixte, 14 Impasse Pierre Baizet, Lyon, F-69263, France.*

[3]*Plateforme Protéome, Centre de Génomique Fonctionnelle, Université de Bordeaux, Bordeaux, France.*

[4]*Department of Plant Pathology, University of Florida, Gainesville, FL.*

[5]*Department of Land, Environment, Agriculture and Forestry (TESAF), Research Group in Plant Pathology, Università degli Studi di Padova, Legnaro, Italy.*

## Summary

**The necrotrophic plant-pathogen fungus *Botrytis cinerea* produces multicellular appressoria dedicated to plant penetration, named infection cushions (IC). A microarray analysis was performed to identify genes upregulated in mature IC. The expression data were validated by RT-qPCR analysis performed *in vitro* and *in planta*, proteomic analysis of the IC secretome and biochemical assays. 1231 upregulated genes and 79 up-accumulated proteins were identified. The data support the secretion of effectors by IC: phytotoxins, ROS, proteases, cutinases, plant cell wall–degrading enzymes and plant cell death–inducing proteins. Parallel upregulation of sugar transport and sugar catabolism–encoding genes would indicate a role of IC in nutrition. The data also reveal a substantial remodelling of the IC cell wall and suggest a role for melanin and chitosan in IC function. Lastly, mutagenesis of two upregulated genes in IC identified secreted fasciclin-like proteins as actors in the pathogenesis of *B. cinerea*. These results support the role of IC in plant penetration and also introduce other unexpected functions for this fungal organ, in colonization, necrotrophy and nutrition of the pathogen.**

Received 28 July, 2020; accepted 28 January, 2021. **For correspondence. E-mail mathias.choquer@univ-lyon1.fr; Tel. +33 472852282. †These authors contributed equally to this work.



## Introduction

Many phytopathogenic fungi differentiate specific structures named appressoria that are dedicated to the penetration of the host tissues (Emmett and Parbery, 1975; Deising *et al*., 2000). Appressoria facilitate the breaching of plant cuticles and cell walls through a mechanical and/or chemical action. Early microscopy studies provided clear observations of these structures in different fungal species and distinguished unicellular appressoria (UA) from multicellular appressoria, referred to as infection cushions (IC) (Emmett and Parbery, 1975). Later, UA have attracted much attention and molecular understanding of their development and function has tremendously increased (Ryder and Talbot, 2015). In contrast, IC remain far less understood at the molecular level, even if a first transcriptomic study of IC in *Fusarium graminearum* has recently been published (Mentges *et al*., 2020).

*Botrytis cinerea* is an ascomycetous fungus that causes grey mould disease on more than 1000 plant species (Elad *et al*., 2016). This disease affects fruits, vegetables and ornamental plants around the world, causing considerable losses every year. It has been ranked among the 10 most severe fungal plant pathogens due to its negative impact on agronomically important crops and on plant products in post-harvest storage. *Botrytis cinerea* is considered a typical necrotrophic fungus and has become a model to study plant infection (Dean *et al*., 2012). It is characterized by its ability to produce either UA or IC *in vitro* or *in planta* (Choquer *et al*., 2007).

The *B. cinerea* IC are multicellular appressoria that develop *in planta* between 24 and 48 h after spore germination. Histological studies have revealed IC from *B. cinerea* on a wide variety of infected plant hosts and organs:

carrot roots (Sharman and Heale, 1977); bean or mung bean hypocotyls (Garcia-Arenal and Sagasta, 1980; Backhouse and Willetts, 1987), bean, cucumber or oilseed rape leaves (Akutsu *et al*., 1981; Van den Heuvel and Waterreus, 1983; Zhang *et al*., 2010), stone fruit or waxflower flowers (Fourie and Holz, 1994; Dinh *et al*., 2011), lemon or persimmon fruits (Fullerton *et al*., 1999; Rheinländer *et al*., 2013) and onion epidermis (Choquer *et al*., 2007). Lastly, *B*. *cinerea* IC also develop *in vitro*, in culture over hard surfaces (Backhouse and Willetts, 1987).

IC have been described in several other Leotiomycetes fungi: *Sclerotinia sclerotiorum* (Tariq and Jeffries, 1984), *Sclerotinia minor* (Lumsden and Wergin, 1980), *Sclerotinia trifoliorum* (Prior and Owen, 1964), *Dumontinia tuberosa* (Pepin, 1980), *Stromatinia cepivora* (Stewart *et al*., 1989) and *Tapesia yallundae* (Daniels *et al*., 1991). In parallel, IC have been described in the Sordariomycetes *Fusarium graminearum* (Boenisch and Schäfer, 2011), and in the Basidiomycota *Athelia rolfsii* (Smith *et al*., 1986), *Rhizoctonia solani* (Demirci and Döken, 1998) and *Rhizoctonia tuliparum* (Gladders and Coley-Smith, 1977).

The recent characterization of several avirulent mutants of *B*. *cinerea* revealed the importance of IC in the infectious process of this necrotrophic fungus (De Vallée *et al*., 2019) and hypo-virulent strains of *B*. *cinerea* infected by mycoviruses are also deficient in IC formation (Zhang *et al*., 2010; Hao *et al*., 2018). Although it has long been accepted that IC mediate penetration, their differentiation, as well as their functions, are still poorly understood. By using a transcriptomic approach, the aim of this study was to provide new molecular information that highlights biological processes (BPs) specifically at work in mature IC of *B*. *cinerea*.

The transcriptomic results, supported by a secretome analysis, are consistent with IC being structures dedicated to the secretion of fungal effectors important for plant penetration and colonization: phytotoxins, ROS, hydrolytic enzymes and plant cell death–inducing proteins (CDIPs). Moreover, the data reveal a deep remodelling of the IC cell wall composition suggesting the importance of melanin and chitosan in the function of IC. The hypothesis of a role for IC in the nutrition of the parasite is also proposed.

## Results

### *Microarray study of IC*

To gain information on the role of IC in the biology of *B*. *cinerea*, we identified genes expressed in these structures. As IC develop onto solid surfaces, potato dextrose agar plates were used for their production while potato dextrose broth was used to produce the control vegetative mycelium. Conidia were used as inoculum, and cellophane sheets were overlaid onto the plates to increase the production of IC and to facilitate their harvest. To obtain as much mature IC as possible, the samples were collected at 44 hpi. At that time, IC were fully differentiated and hyperbranched (Fig. 1), and they covered about 40% of the plates surface (Fig. S1a) while the liquid cultures produced only mycelium (Fig. S1b). Both biological materials were used to extract total RNA and to prepare cDNAs that were hybridized to microarrays carrying probes of 11 134 *B*. *cinerea* genes (Table S1).

Data processing, quality controls and differential expression analysis of the microarrays data led to the listing of 1231 upregulated genes and 1422 downregulated Bcin genes (fold change $\leq -2$ or $\geq 2$; FDR $< 0.05$; Table S1) in the IC-enriched sample (hereafter referred to as IC) when compared with the control vegetative mycelium (13% and 15% of the 9410 expressed genes respectively). The reliability of this result was tested by RT-qPCR analysis. For this, new IC and new control mycelium were produced in order to extract new RNAs. The RT-qPCR reactions were run on 39 genes selected among the upregulated, downregulated and non-

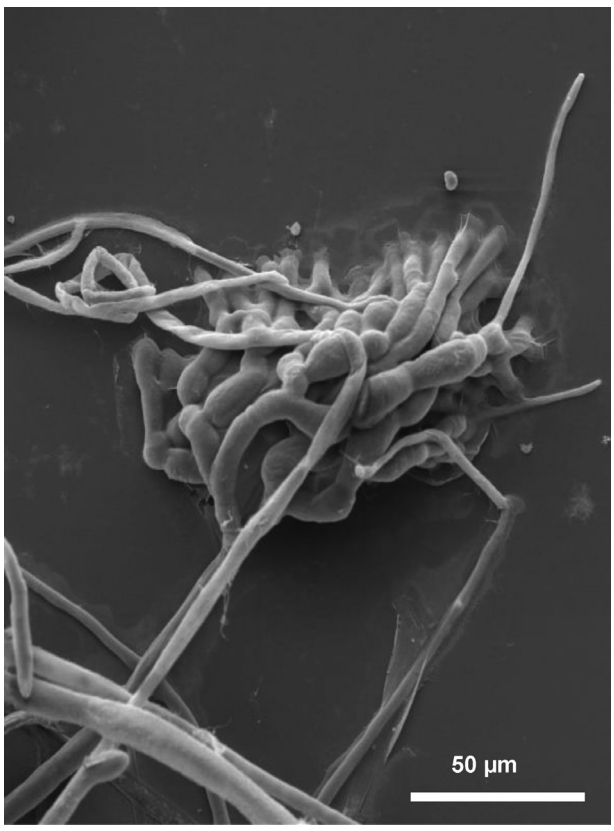


**Fig 1.** Scanning electron microscopy of *Botrytis cinerea* infection cushion. Mature infection cushion, produced on the glass surface, developing multiple and successive ramifications of hyphae (2 dpi).

regulated genes identified by the microarray study (the selection covered genes with different fold-changes). The results confirmed the microarrays data in 85% of the cases (33 genes) and showed no contradiction with the transcriptomic data in the remaining 15% of the cases (Table S2). Altogether, this granted the microarray data a good level of confidence.

### *Functional enrichment analysis of differentially expressed genes in IC*

Enrichment analyses were performed on the upregulated and downregulated genes in IC. By using the gene ontology (GO) BP classification (Gene Ontology; Fig. S2), a significant enrichment was revealed for carbohydrate metabolic process (58 genes), oxidation–reduction process (136 genes), metabolism process (70 genes), transmembrane transport (76 genes) and proteolysis (24 genes). For downregulated genes, rRNA processing (15 genes), ribosome biogenesis (9 genes) and tRNA splicing (five genes) showed enrichment. In order to extract biological meaning from the GO analysis, we used existing databases and published data to manually sort the transcriptional data into 22 functional subcategories (Table S1). Fisher's exact tests confirmed the enrichment of 18 subcategories relating to virulence: plant degradation, production of phytotoxins (and other secondary metabolites) and ROS, plant cell death induction, fungal cell wall remodelling, nutrition and secretion (Table 1).

### *Fungal protein effectors: enzymes degrading the plant tissues and plant CDIPs*

The carbohydrate-active enzymes database (CAZy, Lombard *et al*., 2014) and the classifications of Plant Cell Wall Degrading Enzymes (PCWDE; Van den Brink and de Vries, 2011; Glass *et al*., 2013) were used to subclassify 126 predicted PCWDE-encoding genes in *B*. *cinerea* according to their putative specificity for cellulose (C), hemicellulose (H), pectin (P) or overlapping specificity (H, P or C) (Table S1). As shown in Table 1, genes coding for hemicellulases, pectinases and PCWDE of overlapping specificity were significantly enriched among the upregulated genes in IC, while the genes coding for cellulases were not. Genes coding for cutinases and proteases were also found significantly enriched among the upregulated genes in IC (Table 1). In particular, the aspartyl proteases (Ten Have *et al*., 2010), sedolisins and metallopeptidases subcategories were enriched. Altogether, these results suggest a role for IC in the degradation of the plant barriers and tissues through the production and secretion of hydrolytic enzymes.

In addition, six genes encoding plant CDIPs (Li *et al*., 2020) were upregulated in IC: *BcPg2* and *BcPg3* (Kars *et al*., 2005), *BcXyn11A* (Brito *et al*., 2006), *BcNep2* (Schouten *et al*., 2008), *BcXyg1* (Zhu *et al*., 2017) and the homologue of VmE02 (Nie *et al*., 2019). The subcategory of CDIP is significantly enriched among the upregulated genes in IC (Table 1) and this would suggest that IC actively participate in the triggering of plant cell death.

### *Fungal small molecule effectors: phytotoxins and reactive oxygen species*

Detailed examination of the predicted 42 genes that code for Secondary Metabolism (SM) key enzymes in *B*. *cinerea* B05.10 strain (Table S1; Collado and Viaud, 2016) showed that 11 were upregulated in IC (Table 1; Fig. S3). Noticeably, two SM gene clusters, responsible for the production of botcinic acid and botrydial phytotoxins (Dalmais *et al*., 2011; Porquier *et al*., 2019), were both significantly enriched among the upregulated genes in IC (subcategories '10' and '11' in Table S1; Table 1; Fig. 2A). In addition, the *Bcreg1* gene (Bcin03g07420) encoding the transcriptional regulator required for the synthesis of these toxins (Michielse *et al*., 2011) was also upregulated (Table S1). At last, we observed that five remaining upregulated SM key enzyme-encoding genes are neighboured by genes whose expression was also upregulated in IC, and whose description is compatible with SM typical genes (Fig. S4). This suggests the existence of four additional putative SM clusters transcriptionally induced in *B*. *cinerea* IC. These gene clusters include the *Bcdtc3*, *Bcpks7*, *Bcpks8* or *Bcpks4*/*Bcnrps8* genes.

Detailed examination of the predicted 54 genes that code for ROS-producing systems in *B*. *cinerea* (Siegmund and Viefhues, 2016) showed that 14 were upregulated in IC, making this gene family an enriched subcategory (Table 1; Table S1). These genes encode the catalytic subunit BcNoxB of the NADPH oxidase and its regulator BcNoxR (Segmüller *et al*., 2008), the glucose oxidase BcGod1 (Rolke *et al*., 2004), the galactose oxidase BcGox1, the quinone oxidoreductase BcNqo1 (An *et al*., 2016), as well as three laccases (BcLcc6, 8, 13) and six glucose-methanol-choline oxidoreductases. As ROS play a role in the early phases of plant infection by *B*. *cinerea* (Govrin and Levine, 2000), upregulation of these genes suggested that IC could secrete more ROS than vegetative mycelium. To test this hypothesis, *B*. *cinerea* was cultured for 48 h on liquid PDB medium overlaid with cellophane sheets and the collected culture medium was exposed to 3,3′ diaminobenzidine (DAB) as previously described (Viefhues *et al*., 2014). In comparison with the vegetative mycelium, a stronger oxidation of DAB was observed with the IC culture medium (Fig. 2B), indicating the presence of likely

**Table 1.** Functional enrichment analysis of upregulated genes in the infection cushion of *Botrytis cinerea*.

| Functional subcategories (expert annotation manually curated) | Correspondence with the GO (biological process) | Proposed biological roles | Upregulated genes (1231/11 134) | Enrichment *p*-value | Sources used for curation |
|---|---|---|---|---|---|
| 1: PCWDE*_Cellulose (C) | Carbohydrate metabolic process | Plant degradation | **5**/19 | >5E-2 | CAZy database Lombard *et al*. (2014); www.cazy.org/ Van den Brink and de Vries (2011); Glass *et al*. (2013) |
| 2: PCWDE*_Hemicellulose (H) | | Nutrition | **17**/32 | **5.6E-9** | |
| 3: PCWDE*_Pectin (P) | | | **18**/48 | **1.6E-6** | |
| 4: PCWDE*_C_H_P | | | **13**/26 | **9.1E-7** | |
| 5: FCWE**_Chitin deacetylases (CDA) | | Fungal cell wall remodelling | **3**/5 | **1.2E-2** | Liu *et al*. (2017) |
| 6: Alpha-1,2-mannosidases | | Unknown | **4**/5 | **6.8E-4** | GH92 family in CAZy database |
| 7: ROS-producing systems | Oxidation–reduction process | ROS | **14**/54 | **1.8E-3** | Siegmund and Viefhues (2016); BotPortal database |
| 8: ROS detoxification and scavenging | | | **7**/41 | >5E-2 | |
| 9: Cytochrome P450s | | Phytotoxins, others | **26**/128 | **2.5E-3** | IPR001128*** |
| 10: Botcinic acid biosynthesis genes (Boa) | | Phytotoxins | **10**/10 | **2.7E-10** | Porquier *et al*. (2019) |
| 11: Botrydial biosynthesis genes (Bot) | | | **7**/7 | **5.6E-8** | Dalmais *et al*. (2011) |
| 12: Taurine catabolism dioxygenase TauD/TfdA | | Unknown | **4**/14 | >5E-2 | IPR003819*** |
| 13: Secondary metabolism key enzyme genes (e.g. PKS, NRPS, TS, DMATS) **** | Metabolic process | Phytotoxins, ROS, others | **11**/42 | **4.9E-3** | Collado and Viaud (2016) |
| 14: DHN-melanogenic genes | | Fungal cell wall remodelling | **6**/11 | **5.1E-4** | Schumacher (2016); Cohrs *et al*. (2016) |
| 15: Cutinases | | Plant degradation | **4**/11 | **2.6E-2** | IPR000675*** |
| 16: Sugar transporters | Transmembrane transport | Nutrition | **22**/86 | **1.7E-4** | IPR003663; IPR005829; IPR007271; IPR004689*** |
| 17: Aspartyl proteases | Proteolysis | Plant degradation | **6**/14 | **2.5E-3** | ten Have *et al*. (2010) |
| 18: Sedolisins | | Nutrition | **5**/10 | **2.6E-3** | IPR030400*** |
| 19: Serine carboxypeptidases | | | **4**/16 | >5E-2 | IPR001563, IPR008758, IPR001375*** |
| 20: Metallopeptidases | | | **4**/10 | **1.9E-2** | IPR024079*** |
| 21: Putative secreted proteins (signalP) | All categories | Virulence | **266**/1079 | **8.0E-41** | SignalP-5.0 Almagro Armenteros *et al*. (2019) |
| 22: Plant cell death–inducing proteins (CDIP) | | | **6/**14 | **2.5E-3** | Li *et al*. (2020) |

Functional subcategories were determined according to a GO biological process analysis followed by a manual curation using existing databases and published data. Categories with significant enrichment were identified using Fisher's exact test with a *p*-value cut-off at 0.05 (only the Bcin genes analysed by the chip were used for this test); Number of differentially regulated genes (in bold) and *p*-values are indicated. *PCWDE, Plant cell wall–degrading enzymes; **FCWE, fungus cell wall enzymes; ***Bcin proteins displaying an 'IPR' InterPro domain (www.ebi.ac.uk/interpro/; Mitchell *et al*., 2018) were searched on the BotPortal database (https://bioinfo.bioger.inra.fr/botportalpublic/; Simon and Viaud, 2018); ****PKS, polyketide synthases; NRPS, non-ribosomal peptide synthetases; TS, terpen cyclases; DMATS, dimethylallyl tryptophan synthases.

higher $H_2O_2$ concentration and secretion of peroxidase activity.

### *Melanization and chitin deacetylation remodel the fungus IC cell wall*

In *B. cinerea*, dihydroxynaphthalene-(DHN)-melanins are produced and their biosynthesis relies on a bipartite pathway operating in conidia or in sclerotia (Schumacher, 2016). In conidia, the genes coding for the polyketide synthase BcPks13 and for the hydrolase BcYgh1 are induced by the light transcription factor BcLft2. In sclerotia, the polyketide synthase BcPks12 encoding gene is induced by the transcription factor SMR1 and repressed by BcLtf2 (Cohrs *et al*., 2016). In IC, *Bcpks13*, *Bcygh1*, *Bcltf2* and the other downstream genes of the pathway were upregulated while *Bcpks12* and *Bcsmr1* were downregulated (Fig. 3A–C). This would indicate that IC produce DHN-melanins by using the biosynthetic pathway at play in conidia. Schumacher (2016) proposed laccases

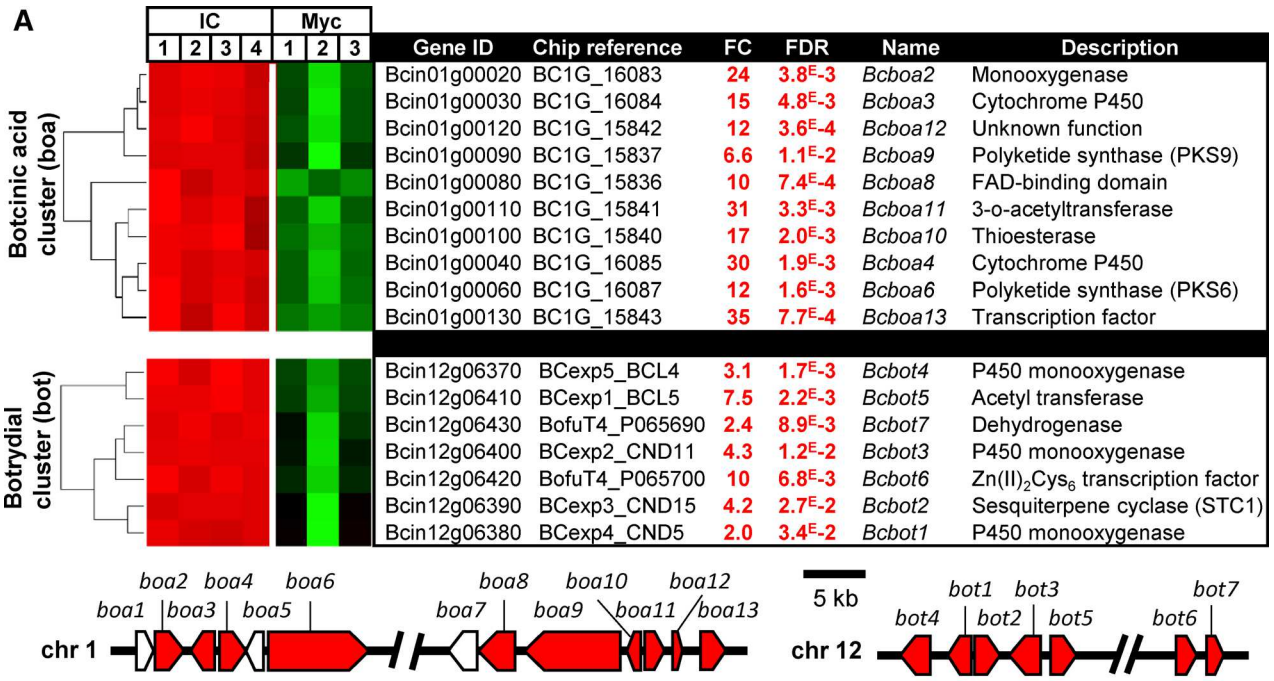


| Gene ID | Chip reference | FC | FDR | Name | Description |
|---|---|---|---|---|---|
| Bcin01g00020 | BC1G_16083 | 24 | $3.8^{E}$-3 | *Bcboa2* | Monooxygenase |
| Bcin01g00030 | BC1G_16084 | 15 | $4.8^{E}$-3 | *Bcboa3* | Cytochrome P450 |
| Bcin01g00120 | BC1G_15842 | 12 | $3.6^{E}$-4 | *Bcboa12* | Unknown function |
| Bcin01g00090 | BC1G_15837 | 6.6 | $1.1^{E}$-2 | *Bcboa9* | Polyketide synthase (PKS9) |
| Bcin01g00080 | BC1G_15836 | 10 | $7.4^{E}$-4 | *Bcboa8* | FAD-binding domain |
| Bcin01g00110 | BC1G_15841 | 31 | $3.3^{E}$-3 | *Bcboa11* | 3-o-acetyltransferase |
| Bcin01g00100 | BC1G_15840 | 17 | $2.0^{E}$-3 | *Bcboa10* | Thioesterase |
| Bcin01g00040 | BC1G_16085 | 30 | $1.9^{E}$-3 | *Bcboa4* | Cytochrome P450 |
| Bcin01g00060 | BC1G_16087 | 12 | $1.6^{E}$-3 | *Bcboa6* | Polyketide synthase (PKS6) |
| Bcin01g00130 | BC1G_15843 | 35 | $7.7^{E}$-4 | *Bcboa13* | Transcription factor |
| Bcin12g06370 | BCexp5_BCL4 | 3.1 | $1.7^{E}$-3 | *Bcbot4* | P450 monooxygenase |
| Bcin12g06410 | BCexp1_BCL5 | 7.5 | $2.2^{E}$-3 | *Bcbot5* | Acetyl transferase |
| Bcin12g06430 | BofuT4_P065690 | 2.4 | $8.9^{E}$-3 | *Bcbot7* | Dehydrogenase |
| Bcin12g06400 | BCexp2_CND11 | 4.3 | $1.2^{E}$-2 | *Bcbot3* | P450 monooxygenase |
| Bcin12g06420 | BofuT4_P065700 | 10 | $6.8^{E}$-3 | *Bcbot6* | $Zn(II)_2Cys_6$ transcription factor |
| Bcin12g06390 | BCexp3_CND15 | 4.2 | $2.7^{E}$-2 | *Bcbot2* | Sesquiterpene cyclase (STC1) |
| Bcin12g06380 | BCexp4_CND5 | 2.0 | $3.4^{E}$-2 | *Bcbot1* | P450 monooxygenase |

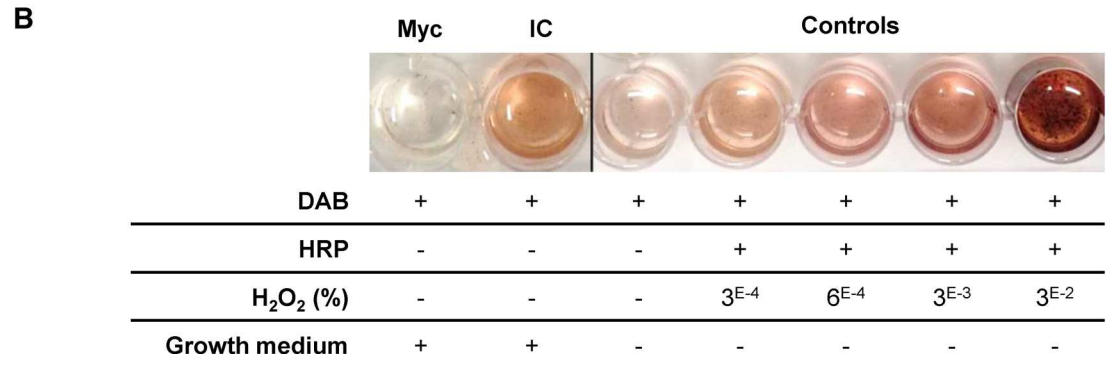


| | | | | | | | |
|---|---|---|---|---|---|---|---|
| **DAB** | + | + | + | + | + | + | + |
| **HRP** | - | - | - | + | + | + | + |
| **$H_2O_2$ (%)** | - | - | - | $3^{E-4}$ | $6^{E-4}$ | $3^{E-3}$ | $3^{E-2}$ |
| **Growth medium** | + | + | - | - | - | - | - |

**Fig 2.** Upregulation of phytotoxins and ROS production in the infection cushion of *Botrytis cinerea*.
A. Hierarchical clustering of the expression of the Botcinic acid genes (*Bcboa*) and botrydial genes (*Bcbot*) in infection cushion. (IC, four biological replicates) and control mycelium (Myc, three biological replicates). The normalized expression intensities are clustered and represented by colour-coded squares; Shades of green and red depict downregulation and upregulation in IC respectively (fold change (FC) ≤ −2 or ≥2 and FDR < 0.05).
Botcinic acid (boa) and botrydial (bot) biosynthesis gene clusters (right; Porquier *et al*., 2019 and Dalmais *et al*., 2011). Genes upregulated in IC are coloured in red. Genes with no chip reference and whose expression could hence not be measured are coloured in white.
B. Visualization of ROS produced by IC. 100 µl of medium was added to 1 ml of DAB and incubated 20 h. Controls were done by adding 1 µl horseradish peroxydase (HRP) to 1 ml DAB in presence of different quantities of $H_2O_2$. The growth medium of 48 h cellophane-overlaid liquid cultures (IC) or agitated liquid cultures (Myc) was mixed into a DAB solution. The oxidation of DAB by $H_2O_2$ in the presence of peroxidases is revealed by a brown coloration. [Color figure can be viewed at wileyonlinelibrary.com]

as potential candidates catalysing the polymerization of DHN-melanins monomers in *B. cinerea*. As *BcLcc6* and *BcLcc8* laccases genes are upregulated in IC, they could eventually play this role (Sapmak *et al*., 2015). In addition, thick dark cell walls were observed in IC (Fig. 3D, top), suggesting that DHN-melanins are deposited at the contact zones between the hyperbranched IC lobes. In the presence of tricyclazole, an inhibitor of the THN reductases BcBrn1 and BcBrn2 (Fig. 3B), hyperbranched IC lobes were still formed but their dark cell walls were not visible anymore. Orange cell walls were observed instead (Fig. 3D, bottom), likely due to the accumulation of T4HN and T3HN and their autooxidation products flaviolin and 2-hydroxyjuglone (Schumacher, 2016). These results confirm the hyper-melanization of IC cell walls and suggest that melanization and hyperbranching are independent processes.

Chitin deacetylases (CDA) are enzymes that produce chitosan from chitin (Fig. 4A). Based on conserved protein

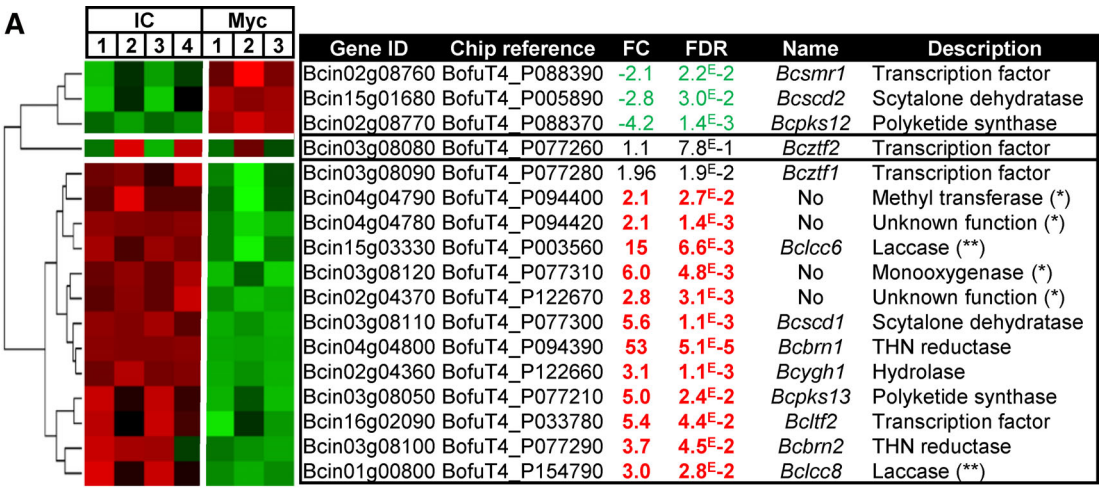


| Gene ID | Chip reference | FC | FDR | Name | Description |
|---|---|---|---|---|---|
| Bcin02g08760 | BofuT4_P088390 | -2.1 | $2.2^{E}$-2 | *Bcsmr1* | Transcription factor |
| Bcin15g01680 | BofuT4_P005890 | -2.8 | $3.0^{E}$-2 | *Bcscd2* | Scytalone dehydratase |
| Bcin02g08770 | BofuT4_P088370 | -4.2 | $1.4^{E}$-3 | *Bcpks12* | Polyketide synthase |
| Bcin03g08080 | BofuT4_P077260 | 1.1 | $7.8^{E}$-1 | *Bcztf2* | Transcription factor |
| Bcin03g08090 | BofuT4_P077280 | 1.96 | $1.9^{E}$-2 | *Bcztf1* | Transcription factor |
| Bcin04g04790 | BofuT4_P094400 | 2.1 | $2.7^{E}$-2 | No | Methyl transferase (*) |
| Bcin04g04780 | BofuT4_P094420 | 2.1 | $1.4^{E}$-3 | No | Unknown function (*) |
| Bcin15g03330 | BofuT4_P003560 | 15 | $6.6^{E}$-3 | *Bclcc6* | Laccase (**) |
| Bcin03g08120 | BofuT4_P077310 | 6.0 | $4.8^{E}$-3 | No | Monooxygenase (*) |
| Bcin02g04370 | BofuT4_P122670 | 2.8 | $3.1^{E}$-3 | No | Unknown function (*) |
| Bcin03g08110 | BofuT4_P077300 | 5.6 | $1.1^{E}$-3 | *Bcscd1* | Scytalone dehydratase |
| Bcin04g04800 | BofuT4_P094390 | 53 | $5.1^{E}$-5 | *Bcbrn1* | THN reductase |
| Bcin02g04360 | BofuT4_P122660 | 3.1 | $1.1^{E}$-3 | *Bcygh1* | Hydrolase |
| Bcin03g08050 | BofuT4_P077210 | 5.0 | $2.4^{E}$-2 | *Bcpks13* | Polyketide synthase |
| Bcin16g02090 | BofuT4_P033780 | 5.4 | $4.4^{E}$-2 | *Bcltf2* | Transcription factor |
| Bcin03g08100 | BofuT4_P077290 | 3.7 | $4.5^{E}$-2 | *Bcbrn2* | THN reductase |
| Bcin01g00800 | BofuT4_P154790 | 3.0 | $2.8^{E}$-2 | *Bclcc8* | Laccase (**) |

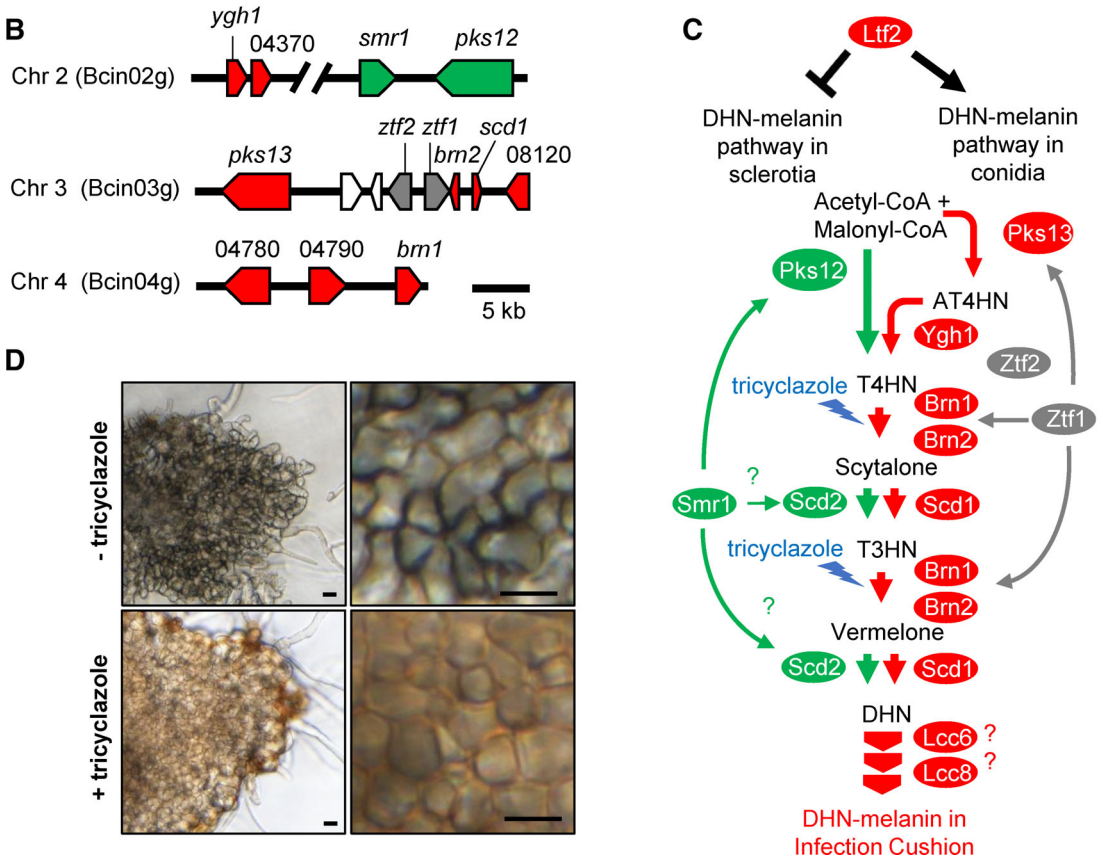


**Fig 3.** Regulation of the DHN melanogenesis bipartite pathway in the infection cushion of *Botrytis cinerea*. This figure is adapted from Schumacher (2016) and Cohrs *et al*. (2016).

A. Hierarchical clustering of the expression of DHN-melanogenic genes in IC (IC, four replicates) and control mycelium (Myc, three replicates) as presented in Fig. 2. Upregulated genes that colocalize with the DHN-melanogenic genes are added for information (*), but their role in melanin biosynthesis remains to be established. Similarly, two laccases upregulated genes (*Bclcc6* and *Bclcc8*) are listed (**) but their role in melanin biosynthesis remains to be established.

B. DHN-melanins biosynthesis putative gene clusters.

C. DHN-melanin metabolic pathway and targets of tricyclazole (lightnings). Genes upregulated or downregulated in IC and corresponding proteins are coloured in red and green respectively.

D. Light microscopy images of hyphae and IC of *B. cinerea* produced on a plastic surface in the absence (top) and presence (bottom) of tricyclazole. Pigmented IC versus hyaline hyphae (left) and dark versus orange-brown thick cell walls inside IC (right) are shown. Bars represent 10 μm. [Color figure can be viewed at wileyonlinelibrary.com]

motifs identified in CDAs (Liu *et al*., 2017), the genome of *B*. *cinerea* putatively encodes five CDA (data not shown). Three of these genes were upregulated in IC when compared with the control mycelium (Fig. 4B; Table S1) while *in planta* RT-qPCR analysis showed upregulation of these five genes at the early phase of bean leaves infection (Fig. 4C). Whether the upregulation of CDA genes impacted the IC cell walls was addressed by using confocal microscopy and differential staining of chitin and chitosan. This allowed the specific visualization of chitosan in IC, hooks and their generating hyphae, but not in the vegetative mycelium (Fig. 4D). This result confirms that some chitin is converted into chitosan in the IC cell wall.

### *Upregulation of sugar uptake and catabolism in IC*

The 'Sugar transporters' subcategory was explored by mining the BotPortal database (https://bioinfo.bioger.inra.fr/botportalpublic/) using the four InterPro domains IPR003663, IPR005829, IPR007271 and IPR004689. This led to the listing of 86 predicted sugar transporters in the genome of *B*. *cinerea* (Table S1), among which 22 were upregulated in IC (Table 1). This upregulation suggests a possible activation of the sugar catabolic pathways and, noticeably, two genes of the glycolysis pathway were upregulated in IC, coding for the fructose-bisphosphate aldolase (Bcin07g03760; Table S1) and the glucose 6-phosphate isomerase *Bcpgi* (Bcin15g04970; Table S1). Besides, in the gluconeogenesis pathway, the *BcPck1* gene (Bcin16g00630; Table S1) encoding the phosphoenolpyruvate carboxykinase was also upregulated in IC. Liu *et al*. (2018) showed that this key gene is crucial for *B*. *cinerea* virulence and for the formation of IC in the absence of glucose. In addition to the enriched metabolic pathways that relate to the degradation of polysaccharides (pectin, glycans), these results suggest an activated sugar catabolism in IC.

### *IC secretome analysis validates the transcriptome analysis*

Of the 1231 upregulated genes in IC, 266 were predicted to code for putative secreted proteins with an N-terminal signal peptide (Table 1 and Table S1) To further investigate these data, the secretomes of IC and control mycelium were compared. *Botrytis cinerea* was grown on cellophane sheets overlaying potato dextrose broth and the culture media were collected at 24 h (control mycelium) or 48 h when IC covered ~40% of the cellophane surface. The proteins were extracted and subjected to a comparative and quantitative proteomics analysis. Seventy nine proteins identified in three biological replicates with a minimum of two unique peptides were listed as up-accumulated (Fold change $\geq$3, FDR < 0.05) in IC (Table 2 and Table S3). Comparison of the proteomics and microarray data (Table S3) showed that 40 of the up-accumulated proteins (51%) are encoded by genes upregulated in IC. By using the GO BP classification, we observed that these secreted proteins are essentially involved in carbohydrate and polysaccharide metabolic processes (27 proteins), proteolysis (16 proteins), oxidation–reduction process (12 proteins) and other metabolic process (two proteins). All these GO categories were found enriched in the analysis of the genes upregulated in IC (Fig. S2). We then used existing databases and published data to manually sort the proteomics data into functional subcategories. We identified virulence-related subcategories similar to those issued from the transcriptome analysis: degradation of plant cuticle, plant cell wall and starch, production of ROS, other degrading enzymes (e.g. nucleases, phosphatases and esterases) and plant cell death–CDIPs. Besides, six CDIP were up-accumulated in the secretome of IC: BcXyn11A (Brito *et al*., 2006), BcNep2 (Schouten *et al*., 2008), BcSpl1 (Frías *et al*., 2013), BcGs1 (Zhang *et al*., 2015), BcIeb1 (Frías *et al*., 2016) and BcXyg1 (Zhu *et al*., 2017). Lastly, a new subcategory enriched in the IC secretome could be identified that corresponds to fungal enzymes implicated in the crosslinking of cell wall polysaccharides. This suggests possible modifications of the covalent links between chitin, glucans and proteins of the IC cell wall. Altogether, the proteomics data support the transcriptomic data and strengthen the signatures of cell wall remodelling and secretion of hydrolytic enzymes or effectors.

### *Relevance of the microarray data to plant infection*

Fourteen upregulated genes in IC whose predicted function relates to pathogenesis were selected for a time-course RT-qPCR analysis *in planta* (bean leaves infected with conidia of *B*. *cinerea*; Fig. 5A and b). All the selected genes were expressed *in planta* suggesting that the microarray data are relevant to plant infection. Twelve of the studied genes were upregulated at days 2, 3 and/or 4 of infection, when IC were visible at the leaf surface. When only hooks could be observed (day 1), most of these genes (11) were not expressed. Furthermore, expression peaked at day 2 for seven genes, when IC were visible, but plant tissue maceration was not. These results suggest that these genes expressed early in IC could play a role in events triggering plant cell death.

### *Fasciclin-like genes upregulated in IC are actors in the virulence of* B. cinerea

Fasciclins play a role in the virulence of the rice pathogen *M*. *oryzae* (Liu *et al*., 2009) via a possible role in the development or in autophagy (Seifert, 2018). In *B*. *cinerea*, two genes encode fasciclin-like proteins (*Bcflp1*;

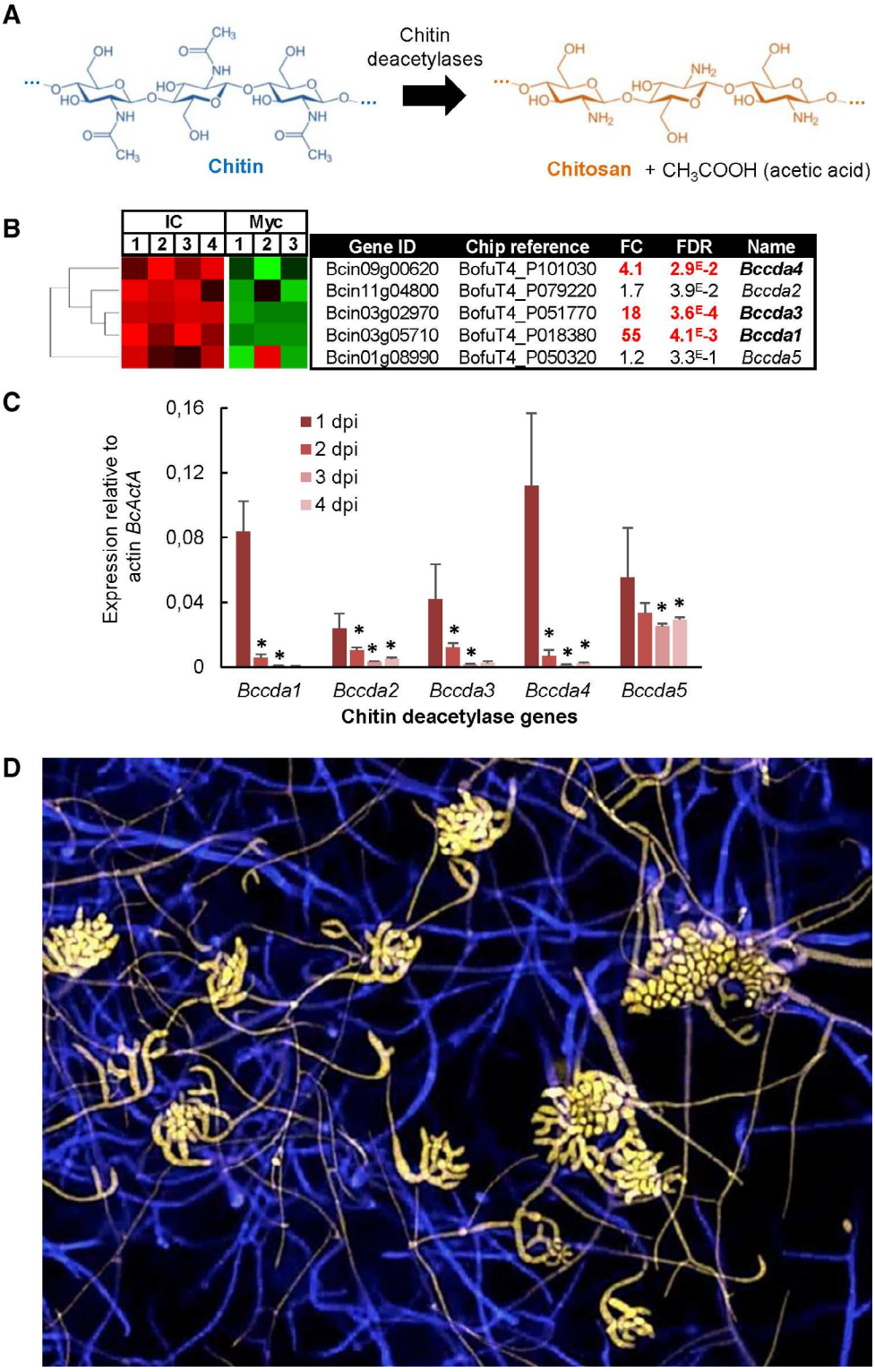


**Fig 4.** Cell wall chitin deacetylation in the infection cushion of *Botrytis cinerea*.
A. Representation of the transformation of chitin into chitosan by chitin deacetylases (cda).
B. Hierarchical clustering of the expression of five putative *cda* genes in infection cushion (IC) and control mycelium (Myc), as presented in Fig. 2.
C. Expression of *Bccda* genes during a kinetics of bean leaves infection by *B. cinerea* (dpi; days post-inoculation). Expression levels were calculated following the $2^{-\Delta\Delta CT}$ method using constitutively expressed actin gene *BcactA* (Bcin16g02020) as a reference. The use of two other
**Fig 4.** Legend on next page.

Bcin04g05020 and *Bcflp2*; Bcin09g05010) and both these genes were upregulated in IC. Following confirmation of this differential expression by RT-qPCR *in vitro* and *in planta* (Table S2; Fig. 5), and since BcFlp1 was up-accumulated in the secretome of IC (Table 2 and Table S3), these two genes were selected for mutagenesis. By using a gene replacement strategy, single-mutant strains (Δ*Bcflp1* and Δ*Bcflp2*) and the double-mutant strain (Δ*Bcflp1*::Δ*Bcflp2*) were constructed. These mutants were genetically purified, and the genotypes were verified by PCR and Southern blotting (Fig. S5). Two independent transformants of each mutant were then characterized. IC formation could be observed in all mutants (data not shown), indicating that the two fasciclin-like proteins are not required for the differentiation of hyphae into IC in *B*. *cinerea*. By contrast, bean leaves infection assays showed that the mutants were affected in their pathogenesis (Fig. 6A and B). In the Δ*Bcflp1* mutant, the colonization rate was similar to that of the wild type but apparition of the symptoms was delayed (estimated at 12 h). In the Δ*Bcflp2* and Δ*Bcflp1*::Δ*Bcflp2* mutants, the colonization rate was reduced and stopped after 4 days. Noticeably, a dark ring was visible at the periphery of the macerated tissues. *In vitro*, neither *Bcflp1* nor *Bcflp2* deletion impaired hyphal growth on rich medium (data not shown). On minimal medium, the Δ*Bcflp2* and Δ*Bcflp1*::Δ*Bcflp2* mutants were moderately impaired in hyphal growth but the Δ*Bcflp1* mutant was not (Fig. 6C). Altogether, the data could indicate that Bcflp1 plays a role during the early stage of the infection process while Bcflp2 could play a role at a later stage. At last, the phenotype of the double mutant indicates a dominant effect of the Δ*Bcflp2* mutation over Δ*Bcflp1*.

## Discussion

### *A role of IC in plant penetration and potential in nutrition*

In plant pathogenic fungi, IC have been proposed to play an important role in host penetration. In this study, four cutinase-encoding genes and 48 predicted PCWDE-encoding genes were revealed as upregulated in *B*. *cinerea* IC. These genes include the endopolygalacturonase *BcPg2* (Bcin14g00610), the endoxylanase *BcXyn11A* (Bcin03g00480) and the endoarabinanase *BcAra1* (Bcin02g07700) required for full virulence of *B*. *cinerea* (Kars *et al*., 2005; Brito *et al*., 2006; Nafisi *et al*., 2014). Besides, aspartyl proteases, sedolisins and metallopeptidases-encoding genes were also significantly upregulated. A proteomic analysis of IC secretome confirmed the up-accumulation of CAZymes and proteases when compared with vegetative mycelium. Altogether, these results support a role for IC in host penetration via enzymatic degradation of plant cell walls.

Unexpectedly, 25 genes coding for sugar transporters and sugar metabolic enzymes were upregulated in IC. In connection with the upregulation of PCWDE-encoding genes, this suggests that IC could play a role in nutrition by importing and catabolizing sugar molecules originating from plant polysaccharides degradation. This would compare to the unicellular appressorium of the rice pathogen *M*. *oryzae* which, besides plant penetration, would also serve to feed on host plant carbohydrates (Soanes *et al*., 2012).

### *A role of IC in establishing necrotrophy?*

Two known SM gene clusters are upregulated in IC. These clusters are responsible for the production of botcinic acid and botrydial, two phytotoxins playing a role in plant infection by *B*. *cinerea* (Cutler *et al*., 1993; Cutler *et al*., 1996; Deighton *et al*., 2001; Dalmais *et al*., 2011; Massaroli *et al*., 2013; Collado and Viaud, 2016). Botrydial sesquiterpene and its derivatives botryanes are proposed as fungal effectors manipulating plant host defences, promoting cell death and thus enabling *B*. *cinerea* to feed on necrotic tissues (Rossi *et al*., 2011). Botcinic acid polyketide and its structurally related botcinins and botrylactones cause plant chlorosis and necrosis (Cutler *et al*., 1993). Double inactivation of these SM clusters led to a defect of pathogenesis and demonstrated the concerted action of the two toxins (Dalmais *et al*., 2011). Interestingly, the coexpression of these clusters in IC supports this concerted action. In addition, four putative SM clusters were also upregulated in IC. The role these clusters might play in virulence and the putative metabolites produced as a result of their activation await characterization. It is noteworthy that several orphan SM have been reported in *B*. *cinerea* while their biosynthesis genes remain unknown (Collado and Viaud, 2016). Additionally, it was proposed that the secretion of new sesquiterpenoid metabolites, called eremophilenols, could promote and regulate the production of *B*. *cinerea* IC, perhaps acting as an endogenous signal (Pinedo *et al*., 2016).

housekeeping genes, elongation factor *Bcef1α* (Bcin09g05760) and pyruvate dehydrogenase *Bcpda1* (Bcin07g01890), gave similar results (data not shown). Three independent biological replicates were assessed for each experiment. Standard errors are displayed, and asterisks indicate a significant difference in gene expression compared with the previous time point (Student's *t*-test, **p*-value <0.05).
D. Confocal microscopy of mycelium and mature IC produced onto a plastic surface at 44 hpi and double-stained with Calcofluor targeting mainly chitin (blue) and Eosin Y targeting mainly chitosan (yellow). [Color figure can be viewed at wileyonlinelibrary.com]

**Table 2.** Up-accumulated proteins in the secretome from the infection cushion of *Botrytis cinerea*.

| Functional category | Subcategory (expert annotation) | Description | Protein ID | Name | FC | *p*-value | Sources used for curation |
|---|---|---|---|---|---|---|---|
| Metabolic process | Plant cuticle degradation | Cutinase (CE5) | Bcin15p00130 | | 54 | 2.2E-12 | IPR000675*** |
| | | | Bcin08p01580 | | 15 | 1.2E-06 | |
| Carbohydrate and polysaccharide metabolic processes | PCWDE* - cellulose | Endo-beta-1,4-glucanase (GH5_5) | Bcin03p04010 | BcCel5A | 4 | 7.3E-03 | Espino *et al*. (2005) |
| | PCWDE* - hemicellulose | **Xylanase (GH11) (CDIP)** | **Bcin03p00480** | **BcXyn11A** | **40** | **7.1E-11** | Brito *et al*. (2006) |
| | | Xylanase (GH10,CBM1) | Bcin05p06020 | BcXyn10B | 5 | 4.3E-03 | García *et al*. (2017) |
| | | Xylosidase (GH31) | Bcin11p06440 | | 3 | 2.8E-02 | CAZy DB**** |
| | PCWDE* - cellulose and hemicellulose | **Xyloglucanase (GH12) (CDIP)** | **Bcin03p03630** | **BcXyg1** | **54** | **2.0E-12** | Zhu *et al*. (2017) |
| | | Xyloglucanase (GH12 CBM1) | Bcin13p02320 | | 53 | 2,3E-12 | CAZy DB**** |
| | PCWDE* - pectin | Rhamnogalacturonan acetylesterase (CE12) | Bcin02p07100 | | 8 | 1.5E-04 | |
| | | Pectin methyl esterase (CE8) | Bcin01p11150 | | 1000 | 9.0E-17 | |
| | | | Bcin08p02970 | BcPme1 | 13 | 4.6E-06 | Kars *et al*. (2005) |
| | Starch degradation (nutrition) | **Glucoamylase (GH15, CBM20) (CDIP)** | **Bcin04p04190** | **BcGs1** | **164** | **9.0E-17** | Zhang *et al*. (2015) |
| | | Glucoamylase (GH15) | Bcin04p00030 | | 19 | 1.7E-07 | CAZy DB**** |
| | | Alpha amylase (GH13) | Bcin02p01420 | | 94 | 2.0E-15 | |
| | | Lytic starch monooxygenase (AA13, CBM20) | Bcin06p05050 | | 33 | 5.4E-10 | Vu *et al*. (2014) |
| | FCWE** remodelling - polysaccharides crosslinking | Beta-1,3-Glucan transferase GAS (GH72) | Bcin02p06940 | BcGas1 | 5 | 3.0E-03 | Patel and Free (2019) |
| | | | Bcin13p02330 | | 3 | 2.7E-02 | CAZy DB**** |
| | | | Bcin14p03970 | | 3 | 2.8E-02 | |
| | | Beta-1,3-Glucan transferase BGL2 (GH17) | Bcin09p00200 | | 15 | 1.2E-06 | |
| | | | Bcin01p11220 | | 5 | 6.1E-03 | |
| | | Alpha-1,6-mannanase Dfg5/ Dcw1 (GH76) | Bcin08p06110 | | 14 | 2.3E-06 | |
| | | Chitin/Glucan transglycosylase CRH (GH16) | Bcin01p06010 | | 8 | 1.9E-04 | |
| | PCWDE* or FCWE**Glucan hydrolysis | Beta glucanase (GH131) | Bcin12p06120 | | 8 | 2.4E-04 | CAZy DB**** |
| | | Beta glucanase (GH131, CBM1) | Bcin09p01150 | | 7 | 3.2E-04 | |
| | | Beta-1,3-glucanase (GH55) | Bcin10p00310 | | 3 | 4.6E-02 | |
| | Other fungal cell wall proteins | WSC domain protein | Bcin15p00810 | | 100 | 9.0E-17 | IPR002889*** |
| | | LysM effector (CBM50) - chitin binding | Bcin02p05630 | BcLysM1 | 28 | 4.2E-09 | Crumière *et al*. (unpublished) |
| | Unknown | Non-classified glycosyl hydrolase (GHnc) | Bcin04p01310 | | 6 | 1.9E-03 | CAZy DB**** |
| | | Putative expansin (CBM63) | Bcin01p02460 | | 5 | 4.3E-03 | |
| Proteolysis | | Aspartic protease | Bcin12p02040 | BcAp8 | 656 | 9.0E-17 | Ten Have *et al*. (2010) |
| | | | Bcin05p05900 | BcAp5 | 25 | 9.9E-09 | |
| | | | Bcin12p00180 | BcAp9 | 19 | 1.8E-07 | |
| | | | Bcin04p02060 | BcAp13 | 4 | 1.2E-02 | |
| | | Sedolisin | Bcin08p01020 | | 1000 | 9.0E-17 | IPR030400*** |
| | | | Bcin15p03150 | | 172 | 9.0E-17 | |
| | | | Bcin15p04670 | BcSer8 | 44 | 2.1E-11 | |

*(Continues)*

 

**Table 2.** Continued

| Functional category | Subcategory (expert annotation) | Description | Protein ID | Name | FC | *p*-value | Sources used for curation |
|---|---|---|---|---|---|---|---|
| | | | Bcin06p00620 | BcTpp2 | 22 | 4.1E-08 | |
| | | | Bcin06p00330 | | 18 | 3.2E-07 | |
| | | | Bcin10p01890 | | 12 | 1.0E-05 | |
| | | Serine carboxypeptidase | Bcin08p00280 | | 269 | 9.0E-17 | IPR001563*** |
| | | | Bcin08p02390 | | 10 | 3.7E-05 | IPR008758*** |
| | | | Bcin06p02510 | | 8 | 2.0E-04 | IPR001375*** |
| | | Metallopeptidase | Bcin16p02770 | BcMp1 | 276 | 9.0E-17 | IPR024079*** |
| | | Glutamic protease | Bcin15p02380 | BcAcp1 | 997 | 9.0E-17 | Billon-Grand *et al*. (2012) |
| | | Putative peptidase S41 | Bcin07p04370 | | 48 | 8.6E-12 | |
| Oxidation-reduction process | ROS producing systems | Glucose-methanol-choline oxidoreductase | Bcin03p01540 | | 53 | 2.7E-12 | Siegmund and Viefhues (2016) |
| | | | Bcin02p07080 | | 16 | 6.3E-07 | BotPortal DBSimon and Viaud (2018) |
| | | | Bcin12p02910 | | 7 | 7.2E-04 | |
| | | Laccase | Bcin14p02510 | BcLcc2 | 1000 | 9.0E-17 | |
| | | | Bcin01p00800 | BcLcc8 | 6 | 1.2E-03 | |
| | ROS detoxification and scavenging | Dyp-type peroxidase | Bcin13p05720 | BcPrd1 | 1000 | 9.0E-17 | |
| | | Peroxidase | Bcin03p07850 | BcPrd10 | 26 | 8.0E-09 | |
| | Other oxidases | Glyoxal oxidase 2 (AA5) | Bcin12p01520 | BcGo2 | 1000 | 9.0E-17 | BotPortal DBSimon and Viaud (2018) |
| | | Putative oxidase | Bcin02p00280 | | 18 | 3.0E-07 | |
| | | | Bcin02p00220 | | 12 | 9.5E-06 | |
| | | | Bcin05p00580 | | 12 | 1.2E-05 | |
| | | | Bcin03p00380 | | 4 | 1.7E-02 | |
| Other or unknown functions | Nucleases | S1/P1 nuclease | Bcin07p06590 | | 81 | 1.2E-14 | Botportal DBSimon and Viaud (2018) |
| | | Ribonuclease T2 | Bcin03p07320 | | 73 | 4.2E-14 | |
| | | | Bcin04p03620 | | 3 | 3.3E-02 | |
| | Phosphatases | Acid phosphatase | Bcin15p03320 | | 15 | 1.2E-06 | |
| | | Phytase subfamily of histidine acid phosphatase | Bcin07p04290 | BcHap1 | 7 | 4.8E-04 | |
| | Esterases | Carboxylesterase | Bcin16p02130 | | 8 | 1.9E-04 | |
| | | Putative esterase | Bcin02p08230 | | 7 | 6.0E-04 | |
| | Other enzymes | Carboxymuconate cyclase | Bcin12p03690 | | 9 | 1.0E-04 | |
| | | Glutamate dehydrogenase | Bcin16p04050 | | 5 | 5.6E-03 | |
| | Other proteins | **Necrosis and ethylene-inducing protein (CDIP)** | **Bcin02p07770** | **BcNep2** | **137** | **9.0E-17** | Schouten *et al*. (2008) |
| | | **Glycoprotein necrosis inducer (CDIP)** | **Bcin15p00100** | **Bcleb1** | **112** | **9.0E-17** | Frías *et al*. (2016) |
| | | **Cerato-platanin family protein (CDIP)** | **Bcin03p00500** | **BcSpl1** | **78** | **1.7E-14** | Frías *et al*. (2013) |
| | | Ubiquitin 3 binding protein But2 | Bcin09p05250 | | 40 | 6.4E-11 | Botportal DB |
| | | Putative Ferritin | Bcin16p03990 | | 18 | 3.0E-07 | |
| | | Fasciclin-like protein | Bcin04p05020 | BcFlp1 | 16 | 8.8E-07 | This study |
| | Hypothetical proteins | | Bcin14p00810 | | 1000 | 9.0E-17 | |
| | | | Bcin06p06670 | | 34 | 5.0E-10 | |
| | | | Bcin09p02890 | | 19 | 1.6E-07 | |

*(Continues)*

**Table 2.** Continued

| Functional category | Subcategory (expert annotation) | Description | Protein ID | Name | FC | *p*-value | Sources used for curation |
|---|---|---|---|---|---|---|---|
| | | | Bcin01p06060 | | 18 | 3.5E-07 | |
| | | | Bcin11p02610 | | 5 | 3.8E-03 | |
| | | | Bcin09p00220 | | 4 | 7.5E-03 | |
| | | | Bcin12p00750 | | 3 | 3.3E-02 | |

Comparison of IC secretome versus mycelium secretome revealed 79 proteins up-accumulated. For quantification, all unique peptides of an identified protein were included, and the total cumulative abundance was calculated by summing the abundances of all peptides allocated to the respective protein. ANOVA test was applied at the protein level. Three independent biological experiments were conducted and analysed. The mass spectrometry proteomics data have been deposited to the ProteomeXchange Consortium via the PRIDE partner repository with the dataset identifier PXD016885. Gene ID and protein accession numbers can be found in Ensembl Fungi release database (http://fungi.ensembl.org/Botrytis_cinerea/Info/Index). The fold change values (FC) between the average protein abundances in the IC and the vegetative mycelia are indicated with the associated *p*-values. The up-accumulated proteins, identified in three biological replicates with a minimum of two unique peptides, are listed and classified according to their functional category (manual annotation). *PCWDE, Plant cell wall–degrading enzymes according to Van den Brink and de Vries (2011) and Glass *et al*. (2013); **FCWE, fungus cell wall enzymes; ***Bcin proteins displaying an 'IPR' InterPro domain (www.ebi.ac.uk/interpro/; Mitchell *et al*., 2018) were searched on the Botportal database (https://bioinfo.bioger.inra.fr/botportalpublic/; Simon and Viaud, 2018); ****CAZy database (Lombard *et al*., 2014; www.cazy.org/). Six plant cell death–inducing proteins (CDIP; Li *et al*., 2020) are shown in bold. (Additional information is provided in Table S3).

During the early phase of plant–fungal interaction, plants produce ROS as part of their defence mechanisms, but ROS are also produced by the pathogen as cell death inducers. In order to produce and cope with ROS, *B. cinerea* is equipped with multiple oxidoreductases. Chemical compounds or mutations that target some of these enzymes, or their encoding genes, impair virulence (Rolke *et al*., 2004; Segmüller *et al*., 2008; An *et al*., 2016; Siegmund and Viefhues, 2016). The analysis of the upregulated genes in IC highlighted 136 genes related to the oxidation–reduction process, among which 15 genes coding for putative ROS-producing enzymes. In addition, higher levels of $H_2O_2$ were detected in IC culture media compared with vegetative mycelium control media. This suggests that IC secretes high amounts of ROS and would therefore be consistent with the production of ROS observed in IC during penetration of onion epidermis (Choquer *et al*., 2007; Marschall and Tudzynski, 2016b). Several gene mutations that impair IC formation in *B. cinerea* have been identified in recent years. Interestingly these genes are often associated with oxidoreduction processes and play a role in the development and virulence of *B. cinerea*. These genes encode the regulator of oxidative stress response BcSkn7 (Viefhues *et al*., 2015), the scaffold protein BcIqg1 involved in resistance against oxidative stress (Marschall and Tudzynski, 2016a), the aquaporin BcAqp8 involved in ROS production (An *et al*., 2016), the ER protein BcPdi1 involved in redox homeostasis (Marschall and Tudzynski, 2017) and the H3K4 demethylase BcJar1 orchestrating ROS production (Hou *et al*., 2020).

During the early phase of plant infection by *B. cinerea*, CDIPs (Qutob *et al*., 2006; Cuesta Arenas *et al*., 2010) could trigger plant cell death from which the fungus would benefit to achieve full virulence (Govrin and Levine, 2000; Govrin *et al*., 2006). Upregulation of CDIP-encoding genes and/or secretion of CDIP have been recorded in *B. cinerea* (Noda *et al*., 2010; Shlezinger *et al*., 2011; Gonzalez *et al*., 2016; Zhu *et al*., 2017). Our study reveals gene upregulation and/or protein up-accumulation for nine of the 14 known CDIPs in *B. cinerea*. Altogether, the upregulation of genes involved in the production of CDIP, phytotoxins and ROS argues for IC playing a role in the establishment of the necrotrophic lifestyle of *B. cinerea*.

In *Colletotrichum* UA, genes encoding effectors and SM enzymes are induced before penetration and during biotrophy while genes encoding most hydrolases and transporters are upregulated later, at the switch to necrotrophy (O'Connell *et al*., 2012). In comparison, the concomitant expression of all these genes recorded herein could also support the role of *B. cinerea* IC in necrotrophy.

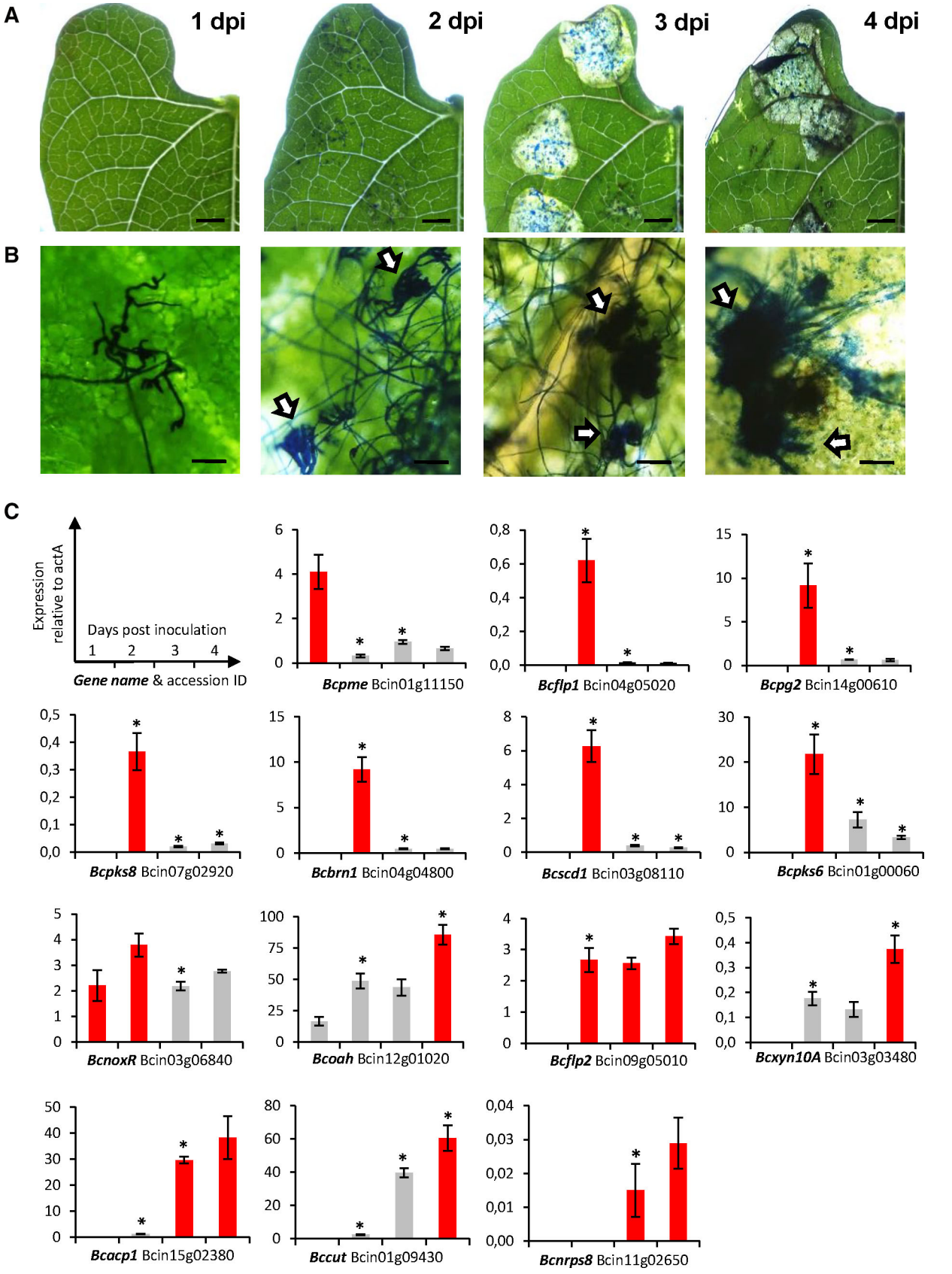


**Fig 5.** Legend on next page.

*Cell wall remodelling in IC*

In *B. cinerea*, cell walls are darkened by DHN-melanins. These pigments are secondary metabolites produced via a bipartite pathway in *B. cinerea*, so far identified as specific to conidia or sclerotia (Schumacher, 2016). The gene expression data reported in this study indicate that the conidial metabolic pathway is activated in IC, while the sclerotial pathway is not. This result suggested that IC produce melanin, as observed in unicellular melanized appressoria (Soanes *et al*., 2012). Microscopic observation of thick dark cell walls in IC that are sensitive to DHN-melanins inhibitors brought experimental support to this. Melanins biosynthesis is dispensable for virulence in *B. cinerea* (Schumacher, 2016) and the reason for their increased production in IC remains to be clarified. It could play a role in the fungus survival during the oxidative burst of host plants (Govrin and Levine, 2000), but it could also play a role in the cross-linking of cell wall components (Franzen *et al*., 2006), the binding of proteins (Mani *et al*., 2001) or that of metals (Fogarty and Tobin, 1996).

Three genes coding for CDA are upregulated in IC. Moreover, differential staining of chitin and chitosan allowed microscopic observations of chitosan in IC and not in vegetative hyphae. This indicates that some chitin is deacetylated into chitosan in the cell wall of IC. Since CDA can play a role in *Aspergillus fumigatus* polar growth (Xie *et al*., 2020) or in *Magnaporthe oryzae* appressorium differentiation (Kuroki *et al*., 2017), the transformation of chitin into chitosan in *B. cinerea* might be involved in the change of hyphal growth that leads to IC formation. Alternatively, the production of chitosan by CDA could play a role in cell wall anchoring of melanins, cell wall integrity, osmotic stability, modulation of extra-cellular polysaccharide production and/or adhesion to surfaces (Baker *et al*., 2007; Geoghegan and Gurr, 2016; Perez-Dulzaides *et al*., 2018; Chrissian *et al*., 2020). At last, chitin deacetylation could prevent detection by the host immune system (Cord-Landwehr *et al*., 2016; Upadhya *et al*., 2018; Lam *et al*., 2019).

Another cell wall–related gene upregulated in *B. cinerea* IC is *Bcsun1* (Bcin06g06040), a beta-glucosidase-encoding gene that is required for full production of IC and full virulence of *B. cinerea* (Pérez-Hernández *et al*., 2017). This adds to the upregulation of the DHN melanin-biosynthesis and the CDA genes, and to the up-accumulation of seven fungal cell wall polysaccharides cross-linking enzymes in the IC secretome. Altogether, this argues for a remodelling of the cell wall in IC.

*Evidencing new putative virulence factors from the IC transcriptome*

Based on the upregulation of their encoding genes in IC, a two-member family of fasciclin-like proteins was selected for functional study. Plant colonization was respectively delayed and arrested in the *Bcflp1* and *Bcflp2* deletion mutants. This suggests a role for these genes in the infection process of *B. cinerea*, at an early stage for *Bcflp1* and at a later stage for *Bcflp2*. As fasciclins could be involved in autophagy in *M. oryzae* and *Schizosaccharomyces pombe* (Liu *et al*., 2009; Sun *et al*., 2013), one may hypothesize a similar function for BcFlp1 and/or BcFlp2, but this needs to be explored.

In a recent study, we collected transcriptomic and proteomic data from four non-pathogenic mutants of *B. cinerea* that do not produce IC (De Vallée *et al*., 2019). Comparison of these data to those presented here showed that 40 of the first 100 upregulated genes in IC are downregulated in all four mutants (Fig. S6). In addition, 47% of the proteins up-accumulated in the culture medium of IC are down-accumulated in the secretome of the four IC-deficient mutants (Table S3). These genes and proteins represent a list of potential virulence factors/effectors in *Botrytis cinerea*.

*Concluding remarks*

This *in vitro* study of IC revealed several enriched categories of upregulated genes (CAZymes, putative effectors, SM,…) that were highlighted in dual-transcriptomes of *B. cinerea* infecting lettuce, tomato, grapevine, cucumber or *Arabidopsis* (Blanco-Ulate *et al*., 2014; Kelloniemi *et al*., 2015; Kong *et al*., 2015; Zhang *et al*., 2019; Zhang *et al*., 2020). It is therefore relevant to plant infection by *B. cinerea*. Interestingly, the recent transcriptome analyses of *F. graminearum* IC developed *in planta* also showed an enrichment of the same categories of genes

**Fig 5.** *In planta* RT-qPCR validation of microarray upregulated genes.
A, B. Infection cushions development on leaves infected by *B. cinerea*. Primary bean leaves were inoculated with conidia and fungal development (1–4 days post-inoculation (dpi)) was monitored using a Stereomicroscope (Zeiss) and cotton blue to stain the fungal cells at the plant surface. IC are pointed by white arrows. Bars represent 5 mm (A) or 50 μm (B).
C. Expression of selected genes during infection. Infected bean leaves were collected to prepare RNAs and RT-qPCR was used to measure the expression of 14 genes upregulated in IC produced *in vitro* conditions (microarray data) and whose predicted function relates to virulence. The red bar indicates the peak of expression for each gene (when two or three bars are in red for the same gene, statistics cannot distinguish them). Gene expression levels were calculated following the $2^{-\Delta\Delta CT}$ method using constitutively expressed actin gene *BcactA* (Bcin16g02020) as a reference. The use of two other housekeeping genes, elongation factor *Bcef1α* (Bcin09g05760) and pyruvate dehydrogenase *Bcpda1* (Bcin07g01890), showed similar results (data not shown). Standard errors of three independent biological replicates are displayed and asterisks indicate a significant difference in gene expression compared with the previous time point (Student's *t*-test, *p*-value <0.05). [Color figure can be viewed at wileyonlinelibrary.com]

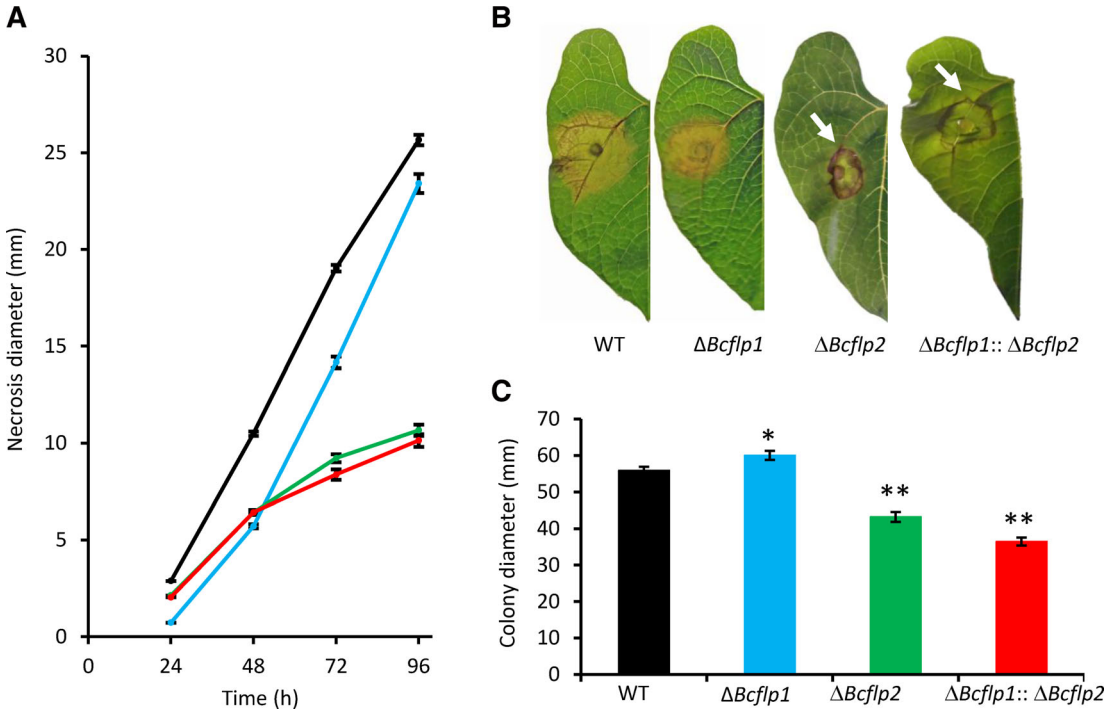


**Fig 6.** Characterization of fasciclin-like deletion mutants in *Botrytis cinerea*.
A. Infection kinetics - French bean leaves were inoculated with mycelial plugs of the WT and deletion strains. The necrosis of the plant tissues was measured every 24 h (at least eight plants and 32 infection points) over 4 days in three independent experiments. Bars indicate standard errors.
B. Visualization of the necrotic lesions. At 72 h post-inoculation, typical images of bean leaves infected by the WT and mutant strains are presented. White arrows indicate dark rings at the edge of the necrotic zones.
C. Growth *in vitro*: The WT strain, the single mutant strains (Δ*Bcflp1* and Δ*Bcflp2*) and the double mutant strain (Δ*Bcflp1*::Δ*Bcflp2*) were grown on a minimal medium for 72 h. The diameters of the colonies were measured on four independent experiments conducted with five plates for each strain. Bars indicate standard errors and stars indicate significant differences (Student *t*-test, *p*-value <0.05) between the WT and the mutants. Similar results were recorded for all experiments on two independent strains of each mutant. [Color figure can be viewed at wileyonlinelibrary.com]

(Mentges *et al*., 2020) and suggest that IC might share conserved virulence functions in different plant pathogenic fungi.

## Experimental procedures

### *Fungal strains and growth conditions*

*Botrytis cinerea* B05.10 conidia were collected in PDB medium (Difco) diluted one-fourth (PDB¼), after 10 days of culture on malt sporulation medium, at 21°C under near-UV light. All subsequent cultures were done in the dark at 21°C. For IC formation, $2 \times 10^5$ conidia were spread onto cellophane sheets overlaying PDB¼ medium supplemented with agar (25 g $l^{-1}$), and the plates were incubated for 44 h. For the control sample, $2 \times 10^5$ conidia were inoculated in 50 ml PDB¼ medium and the 250 ml flasks were agitated (110 rpm) for 44 h. The flasks were previously siliconized with Sigmacote (Sigma) to prevent mycelium adhesion and IC formation on the glassware. For radial growth measurements, wild-type and mutant strains were grown on minimal medium ($NaNO_3$ 2 g $L^{-1}$, Glucose 20 g $L^{-1}$, $KH_2PO_4$ 0.2 g $L^{-1}$, $MgSO_4$, $7H_2O$ 0.1 g $L^{-1}$, KCl 0.1 g $L^{-1}$, $FeSO_4$, $7H_2O$ 4 mg $L^{-1}$). For secretome analysis, $2 \times 10^5$ conidia were spread onto cellophane membrane overlaying solid PDB¼. After 6 h incubation (21°C), membranes were transferred on 2 ml liquid PDB¼ for 24 h (Control mycelium condition) or 48 h (IC condition) at 21°C. Liquid medium was then collected for proteomic analysis. For microscopy, $10^4$ conidia or single mycelial plug served to inoculate PDB¼ medium in six-well microplates. The plates were incubated 44 h at 21°C in the dark.

### *Microarray expression analysis*

To study the transcriptome of *B. cinerea*, NimbleGen 4-plex arrays containing $4 \times 72\,000$ arrays per slide were used (Roche, Mannheim, Germany). Construction of this chip was initially based on combining two previous genome annotations (Amselem *et al*., 2011), the one of the T4 strain by URGI (BofuT4 gene references;

https://urgi.versailles.inra.fr) and the one of the B05.10 strain by the Broad Institute (BC1G gene references; www.broadinstitute.org). Thus, 62 478 60-mer oligonucleotides were designed as specific probes covering 20 885 predicted gene models and non-mapping expressed sequence tags (EST) (three oligonucleotides per gene or EST) and 9559 random probes were designed as negative controls.

The structural annotation used for this study was published by van Kan *et al*. (2017), displaying 11 710 predicted genes, associated with 13 749 predicted proteins, unlike the two previous annotations showing more than 16 000 predicted genes (BofuT4 and BC1G). This annotation is considered better on the basis of RNA-seq data and is available at EnsemblFungi under the reference *Botrytis cinerea* B05.10 (ASM83294v1; Bcin gene references; http://fungi.ensembl.org/Botrytis_cinerea/). 11 710 Bcin genes are predicted but not all of them were analysed by the *B. cinerea* NimbleGen 4-plex arrays. In order to associate each BofuT4 and BC1G gene from the chip to only one Bcin gene and reciprocally, we used the correspondence established in the *B. cinerea* Portal (Simon and Viaud, 2018; https://bioinfo.bioger.inra.fr/botportalpublic/). In a hundred of cases, BofuT4/BC1G genes showing correspondence with multiple Bcin genes were checked by gene synteny. After this manual curation, we identified 11 630 BofuT4/BC1G genes out of 15 750 showing correspondence with only one Bcin gene. When a Bcin gene showed correspondence with multiple BofuT4/ BC1G genes, we selected the BofuT4 or BC1G gene giving the highest normalized intensities. After these two manual curations, we found that 11 134 Bcin genes were analysed by the chip which represent 95% of the published Bcin genes (11 710; Table S1). The EST and the small coding sequences (<100 amino acids) lacking EST support were excluded from our analysis.

Total RNA was extracted from 4 mg of ground lyophilized material using the RNeasy Midi kit (Qiagen). A DNase treatment (Ambion) was performed to remove traces of genomic DNA. RNA profiles were assessed using the Bioanalyzer RNA 6000 Nano kit (Agilent). Ten micrograms of total RNA were converted into cDNA using the SuperScript II cDNA Conversion Kit (Invitrogen). Double-stranded cDNAs were then labelled with Cy3-nonamers using NimbleGen One-Colour DNA Labeling Kit before hybridization on the NimbleGen 4-plex arrays. Microarrays were then scanned with an Agilent scanner at 532 nm (Cy3 absorption peak) optimized for Nimblegen 4-plex arrays. All steps were performed following the procedures established by NimbleGen. The entire microarray dataset described in this article is available at the Gene Expression Omnibus database under accession number GSE141822.

Data processing, quality controls, differential expression analysis and clustering were performed using ANAIS methods (Simon and Biot, 2010). Hybridization signals of all probes, comprising three and four independent replicates for mycelium condition and infection cushion condition respectively, were subjected to RMA-background correction, quantile normalization and gene summarization. Thresholds of gene expression were determined by referring the hybridization signals to those of 9559 random probes, calculated for each array using the R software (R Core Team, 2019). Genes were considered expressed when their normalized intensity was higher than the 99th percentile of random probes hybridization signals in at least one biological replicate. These genes were kept for differential expression analysis. Differentially expressed genes, between the infection cushion condition and the mycelium condition, were identified using a one-way ANOVA test. To deal with multiple testings, the ANOVA *p*-values were submitted to a false discovery rate (FDR) correction. Transcripts with a corrected *p*-value <0.05 and for which a fold change $\leq -2$ or $\geq 2$ was observed between the two conditions were considered to display significant differential expression. Clusters analyses of gene normalized intensities were performed to highlight differentially expressed genes.

### *Enrichment analysis and genes categorization*

Further analyses were performed to highlight BPs potentially enriched in the selected lists of upregulated or downregulated Bcin genes in infection cushion. Enrichment in GO BP terms was assessed on the *Botrytis cinerea* B05.10 (ASM83294v1) species using the Fungifun website (Priebe *et al*., 2015; https://elbe.hki-jena.de/fungifun/). The background dataset of genes used as reference was the 11 134 Bcin genes that were associated with the chip (Table S1). The presence of a putative signal peptide was predicted using the SignalP 5.0 Server (Almagro Armenteros *et al*., 2019). The CAZy database (www.cazy.org) was used for the manual curation of PCWDE and the alpha-1,2-mannosidases. The InterPro database (www.ebi.ac.uk/interpro/; Mitchell *et al*., 2018) and the BotPortal database (https://bioinfo.bioger.inra.fr/botportalpublic/; Simon and Viaud, 2018) were used for the manual curation of cytochrome P450s, taurine catabolism dioxygenases, cutinases, sugar transporters, sedolisins, serine carboxypeptidases and metallopeptidases. Functional categories with significant enrichment were identified using Fisher's exact test with a *p*-value cut-off at 0.05 (only the Bcin genes analysed by the chip were used for this test).

### *Expression profiling by quantitative PCR analysis*

Experiments were performed as described by Rascle *et al*. (2018). RT-qPCR experiments were performed using ABI-7900 Applied Biosystems (Applied Biosystems).

Amplification reactions were carried out using SYBR Green PCR Master Mix (Applied Biosystems). Relative quantification was based on the 2(−ΔΔC(T)) method (Livak and Schmittgen, 2001) using the *BcactA* (Bcin16g02020), *Bcef1α* gene (Bcin09g05760) and *Bcpda1* gene (Bcin07g01890) as normalization internal controls. At least three independent biological replicates were analysed. Primers used for RT-qPCR are shown in Table S4.

### *ROS and melanin production*

For visualization of melanin, a stock solution of the DHN melanogenesis inhibitor tricyclazole (Sigma) was prepared in acetone (10 mg $ml^{-1}$). Three-day-old 2-mm mycelial plugs were deposited in six-well plates. Droplets (50 µl) of PDB¼ (supplemented or not with 50 µg $ml^{-1}$ tricyclazole) medium were added on the plugs. After 48 h incubation (21°C), IC were observed by reverse microscopy. For visualization of ROS produced during IC formation, 100 µl of medium were added to 1 ml of DAB (Sigma) solution (0.05% in 100 mM citric acid buffer pH 3.7) and incubated 20 h in darkness with gentle agitation. Controls were done by adding 1 µl horseradish peroxydase (HRP - Thermoscientific) to 1 ml DAB in presence of different quantities of $H_2O_2$.

### *Quantitative proteomic analysis*

The steps of sample preparation and protein digestion were performed as previously described (Dieryckx *et al*., 2015) and online nanoLC–MS/MS analyses were performed using an Ultimate 3000 RSLC Nano-UPHLC system (Thermo Scientific) coupled to a nanospray Q Exactive hybrid quadrupole-Orbitrap mass spectrometer (Thermo Scientific). The parameters of the LC–MS method used were as previously described (Pineda *et al*., 2018). Protein identification and label-free quantification (LFQ) were done in Proteome Discoverer 2.3. MS Amanda 2.0, Sequest HT and Mascot 2.4 algorithms were used for protein identification in batch mode by searching against the Ensembl *Botrytis cinerea* B05.10 database (ASM83294v1, 13 749 entries, release 98.3). Two missed enzyme cleavages were allowed. Mass tolerances in MS and MS/MS were set to 10 ppm and 0.02 Da. Oxidation (M), acetylation (K) and deamidation (N, Q) were searched as dynamic modifications and carbamidomethylation (C) as static modification. Peptide validation was performed using Percolator algorithm (Käll *et al*., 2007) and only 'high confidence' peptides were retained, corresponding to a 1% FDR at peptide level. Minora feature detector node (LFQ) was used along with the feature mapper and precursor ions quantifier. The normalization parameters were selected as follows: (i) unique peptides, (ii) precursor abundance based on intensity, (iii) normalization mode: total peptide amount, (iv) protein abundance calculation: summed abundances, (v) protein ratio calculation: pairwise ratio based and (vi) Hypothesis test: *t*-test (background based). Quantitative data were considered for master proteins, quantified by a minimum of two unique peptides, a fold change ≥3 and a statistical *p*-value lower than 0.05. The mass spectrometry proteomics data have been deposited to the ProteomeXchange Consortium (http://proteomecentral.proteomexchange.org) via the PRIDE partner repository (Perez-Riverol *et al*., 2019) with the dataset identifier PXD016885.

### *Construction of deletion mutants in* Botrytis cinerea

Δ*Bcflp1* and Δ*Bcflp2* deletion mutants were constructed using a gene replacement strategy (Fig. S5). The replacement cassettes were generated by combining double-joint PCR (Yu *et al*., 2004) and split-marker approach (Catlett *et al*., 2003). All primers are listed in Table S4. The three gene replacement cassettes were verified by sequencing. *Botrytis cinerea* transformation was carried out using protoplasts as previously described by Rascle *et al*. (2018), except that the protoplasts were transformed with 1 µg of each split-marker cassette DNA and plated on medium containing 200 g $L^{-1}$ saccharose and 2 g $L^{-1}$ $NaNO_3$ supplemented with 70 µg $ml^{-1}$ hygromycin (Invivogen, France) for single Δ*Bcflp1* or Δ*Bcflp2* mutants or 80 µg $ml^{-1}$ nourseothricin (Werner BioAgents, Germany) for double-replacement mutants. Diagnostic PCR was performed to detect homologous recombination in the selected resistant transformants. Homokaryotic transformants were obtained after several rounds of single-spore isolation. Southern blot analyses were performed to ensure single insertions. Genomic DNA digested with *Eco*RI was hybridized with the 3′- flanking region of *Bcflp1* (amplified with Probe1For and Probe1Rev primers) or the 5′-flanking region of *Bcflp2* (amplified with Probe2For and Probe2Rev primers) using the PCR DIG Probe Synthesis Kit and the DIG Luminescent Detection Kit (Roche) following the manufacturer's instructions.

### *Pathogenicity tests*

Infection assays were performed with 1-week-old French bean (*Phaseolus vulgaris* var *Saxa*) leaves using 4-mm fresh mycelial plugs from *B. cinerea* WT, Δ*Bcflp1*, Δ*Bcflp2* and Δ*Bcflp1*::Δ*Bcflp2* mutant strains grown on sporulation medium. Infected plants were incubated at 21°C under 100% relative humidity and dark (10 h)-daylight (14 h) conditions. Necrosis zone diameter was measured daily. All tests were assessed in three

independent experiments, with at least eight plants and 30 points of infection for each strain.

### *Microscopy*

Confocal microscopy and imaging were performed with a Zeiss LSM510 confocal microscope (Oberkochen, Germany) and its integrated ZEN software. For staining of chitin and chitosan, the fungal culture medium was drained and replaced by 1 ml $H_2O$ containing 20 µl KOH 10%, 10 µl Calcofluor (Fluka, 1 g $L^{-1}$) and 10 µl eosin Y 0.5% (Sigma). Following 10 min incubation in the dark, the staining solution was drained, the samples were washed five times with 1 ml $H_2O$ and overlaid with 0.5 ml $H_2O$. Fluorescent signals of calcofluor and eosin Y were respectively captured using a 405 and 561 nm excitation wavelength.

## Acknowledgements

We thank Adeline Simon, Lucile Albinet and Luna Nadjare for providing tools and help on bioinformatic analyses. We thank Gwenlyn Fleury for her implication in the study of fasclicin mutants, and Cindy Dieryckx and Vincent Girard for their advice on secretome analysis. We are thankful to Glen Calvar for English editing.

## References

Akutsu, K., Kobayashi, Y., Matsuzawa, Y., Watanabe, T., Ko, K., and Misato, T. (1981) Morphological studies on infection process of cucumber leaves by conidia of *Botrytis cinerea* stimulated with various purine-related compounds. *Jpn J Phytopathol* **47**: 234–243.

Almagro Armenteros, J.J., Tsirigos, K.D., Sønderby, C.K., Petersen, T.N., Winther, O., Brunak, S., *et al*. (2019) SignalP 5.0 improves signal peptide predictions using deep neural networks. *Nat Biotechnol* **37**: 420–423.

Amselem, J., Cuomo, C.A., van Kan, J.A.L., Viaud, M., Benito, E.P., Couloux, A., *et al*. (2011) Genomic analysis of the necrotrophic fungal pathogens *Sclerotinia sclerotiorum* and *Botrytis cinerea*. *PLoS Genet* **7**: e1002230.

An, B., Li, B., Li, H., Zhang, Z., Qin, G., and Tian, S. (2016) Aquaporin8 regulates cellular development and reactive oxygen species production, a critical component of virulence in *Botrytis cinerea*. *New Phytol* **209**: 1668–1680.

Backhouse, D., and Willetts, H.J. (1987) Development and structure of infection cushions of *Botrytis cinerea*. *Trans Br Mycol Soc* **89**: 89–95.

Baker, L.G., Specht, C.A., Donlin, M.J., and Lodge, J.K. (2007) Chitosan, the deacetylated form of chitin, is necessary for cell wall integrity in *Cryptococcus neoformans*. *Eukaryot Cell* **6**: 855–867.

Billon-Grand, G., Rascle, C., Droux, M., Rollins, J.A., and Poussereau, N. (2012) pH modulation differs during sunflower cotyledon colonization by the two closely related necrotrophic fungi *Botrytis cinerea* and *Sclerotinia sclerotiorum*: *Botrytis* and *Sclerotinia* differ in pH modulation. *Mol Plant Pathol* **13**: 568–578.

Blanco-Ulate, B., Morales-Cruz, A., Amrine, K.C.H., Labavitch, J.M., Powell, A.L.T., and Cantu, D. (2014) Genome-wide transcriptional profiling of *Botrytis cinerea* genes targeting plant cell walls during infections of different hosts. *Front Plant Sci* **5**: 435.

Boenisch, M.J., and Schäfer, W. (2011) *Fusarium graminearum* forms mycotoxin producing infection structures on wheat. *BMC Plant Biol* **11**: 110.

Brito, N., Espino, J.J., and González, C. (2006) The Endo-β-1,4-Xylanase Xyn11A is required for virulence in *Botrytis cinerea*. *MPMI* **19**: 25–32.

Catlett, N.L., Lee, B.-N., Yoder, O.C., and Turgeon, B.G. (2003) Split-marker recombination for efficient targeted deletion of fungal genes. *Fungal Genet Rep* **50**: 9–11.

Choquer, M., Fournier, E., Kunz, C., Levis, C., Pradier, J.-M., Simon, A., and Viaud, M. (2007) *Botrytis cinerea* virulence factors: new insights into a necrotrophic and polyphageous pathogen. *FEMS Microbiol Lett* **277**: 1–10.

Chrissian, C., Camacho, E., Fu, M.S., Prados-Rosales, R., Chatterjee, S., Cordero, R.J.B., *et al*. (2020) Melanin deposition in two *Cryptococcus* species depends on cell-wall composition and flexibility. *J Biol Chem* **295**: 1815–1828.

Cohrs, K.C., Simon, A., Viaud, M., and Schumacher, J. (2016) Light governs asexual differentiation in the grey mould fungus *Botrytis cinerea* via the putative transcription factor BcLTF2: BcLTF2 regulates conidiation in *Botrytis cinerea*. *Environ Microbiol* **18**: 4068–4086.

Collado, I.G., and Viaud, M. (2016) Secondary metabolism in *Botrytis cinerea*: combining genomic and metabolomic approaches. In *Botrytis – The Fungus, the Pathogen and Its Management in Agricultural Systems*, Fillinger, S., and Elad, Y. (eds). Cham: Springer International Publishing, pp. 291–313.

Cord-Landwehr, S., Melcher, R.L.J., Kolkenbrock, S., and Moerschbacher, B.M. (2016) A chitin deacetylase from the endophytic fungus *Pestalotiopsis* sp. efficiently inactivates the elicitor activity of chitin oligomers in rice cells. *Sci Rep* **6**: 38018.

Cuesta Arenas, Y., Kalkman, E.R.I.C., Schouten, A., Dieho, M., Vredenbregt, P., Uwumukiza, B., *et al*. (2010) Functional analysis and mode of action of phytotoxic Nep1-like proteins of *Botrytis cinerea*. *Physiol Mol Plant Pathol* **74**: 376–386.

Cutler, H.G., Jacyno, J.M., Harwood, J.S., Dulik, D., Goodrich, P.D., and Roberts, R.G. (1993) Botcinolide: a biologically active natural product from *Botrytis cinerea*. *Biosci Biotechnol Biochem* **57**: 1980–1982.

Cutler, H.G., Parker, S.R., Ross, S.A., Crumley, F.G., and Schreiner, P.R. (1996) Homobotcinolide: a biologically active natural homolog of Botcinolide from *Botrytis cinerea*. *Biosci Biotechnol Biochem* **60**: 656–658.

Dalmais, B., Schumacher, J., Moraga, J., Le Pêcheur, P., Tudzynski, B., Collado, I.G., and Viaud, M. (2011) The *Botrytis cinerea* phytotoxin botcinic acid requires two polyketide synthases for production and has a redundant role in virulence with botrydial: Botcinic acid biosynthesis gene clusters. *Mol Plant Pathol* **12**: 564–579.

Daniels, A., Lucas, J.A., and Peberdy, J.F. (1991) Morphology and ultrastructure of W and R pathotypes of *Pseudocercosporella herpotrichoides* on wheat seedlings. *Mycol Res* **95**: 385–397.

De Vallée, A., Bally, P., Bruel, C., Chandat, L., Choquer, M., Dieryckx, C., *et al*. (2019) A similar secretome disturbance as a hallmark of non-pathogenic *Botrytis cinerea* ATMT-mutants? *Front Microbiol* **10**: 2829.

Dean, R., Van Kan, J.A.L., Pretorius, Z.A., Hammond-Kosack, K.E., Di Pietro, A., Spanu, P.D., *et al*. (2012) The top 10 fungal pathogens in molecular plant pathology. *Mol Plant Pathol* **13**: 414–430.

Deighton, N., Muckenschnabel, I., Colmenares, A.J., Collado, I.G., and Williamson, B. (2001) Botrydial is produced in plant tissues infected by *Botrytis cinerea*. *Phytochemistry* **57**: 689–692.

Deising, H.B., Werner, S., and Wernitz, M. (2000) The role of fungal appressoriain plant infection. *Microbes Infect* **2**: 1631–1641.

Demirci, E., and Döken, M.T. (1998) Host penetration and infection by the anastomosis groups of *Rhizoctonia solani Kühn* isolated from potatoes. *Turk J Agric For* **22**: 609–613.

Dieryckx, C., Gaudin, V., Dupuy, J.-W., Bonneu, M., Girard, V., and Job, D. (2015) Beyond plant defense: insights on the potential of salicylic and methylsalicylic acid to contain growth of the phytopathogen *Botrytis cinerea*. *Front Plant Sci* **6**: 859.

Dinh, S.Q., Joyce, D.C., Irving, D.E., and Wearing, A.H. (2011) Histology of waxflower (*Chamelaucium* spp.) flower infection by *Botrytis cinerea*. *Plant Pathol* **60**: 278–287.

Elad, Y., Pertot, I., Prado, A.M.C., and Stewart, A. (2016) Plant hosts of *Botrytis* spp. In Botrytis–The Fungus, the Pathogen and Its Management in Agricultural Systems: Cham: Springer, pp. 413–486.

Emmett, R.W., and Parbery, D.G. (1975) Appressoria. *Annu Rev Phytopathol* **13**: 147–165.

Espino, J.J., Brito, N., Noda, J., and González, C. (2005) *Botrytis cinerea* endo-ß-1,4-glucanase Cel5A is expressed during infection but is not required for pathogenesis. *Physiol Mol Plant Pathol* **66**: 213–221.

Fogarty, R.V., and Tobin, J.M. (1996) Fungal melanins and their interactions with metals. *Enzyme Microb Technol* **19**: 311–317.

Fourie, J.F., and Holz, G. (1994) Infection of plum and nectarine flowers by *Botrytis cinerea*. *Plant Pathol* **43**: 309–315.

Franzen, A.J., Cunha, M.M.L., Batista, E.J.O., Seabra, S.H., De Souza, W., and Rozental, S. (2006) Effects of tricyclazole (5-methyl-1,2,4-triazol[3,4] benzothiazole), a specific DHN–melanin inhibitor, on the morphology of *Fonsecaea pedrosoi* conidia and sclerotic cells. *Microsc Res Tech* **69**: 729–737.

Frías, M., Brito, N., and González, C. (2013) The *Botrytis cinerea* cerato-platanin BcSpl1 is a potent inducer of systemic acquired resistance (SAR) in tobacco and generates a wave of salicylic acid expanding from the site of application. *Mol Plant Pathol* **14**: 191–196.

Frías, M., González, M., González, C., and Brito, N. (2016) BcIEB1, a *Botrytis cinerea* secreted protein, elicits a defense response in plants. *Plant Sci* **250**: 115–124.

Fullerton, R.A., Harris, F.M., and Hallett, I.C. (1999) Rind distortion of lemon caused by *Botrytis cinerea* Pers. *N Z J Crop Hortic Sci* **27**: 205–214.

García, N., González, M.A., González, C., and Brito, N. (2017) Simultaneous silencing of Xylanase genes in *Botrytis cinerea*. *Front Plant Sci* **8**: 2174.

Garcia-Arenal, F., and Sagasta, E.M. (1980) Scanning electron microscopy of *Botrytis cinerea* penetration of bean (*Phaseolus vulgaris*) hypocotyls. *Phytopathol Z* **99**: 37–42.

Geoghegan, I.A., and Gurr, S.J. (2016) Chitosan mediates germling adhesion in *Magnaporthe oryzae* and is required for surface sensing and germling morphogenesis. *PLoS Pathog* **126**: e1005703.

Gladders, P., and Coley-Smith, J.R. (1977) Infection cushion formation in *Rhizoctonia tuliparum*. *Trans Br Mycol Soc* **68**: 115–118.

Glass, N.L., Schmoll, M., Cate, J.H.D., and Coradetti, S. (2013) Plant cell wall deconstruction by Ascomycete fungi. *Annu Rev Microbiol* **67**: 477–498.

Gonzalez, C., Brito, N., and Sharon, A. (2016) Infection process and fungal virulence factors. In Botrytis - The Fungus, the Pathogen and Its Management in Agricultural Systems, pp. 229–246. Cham: Springer.

Govrin, E.M., and Levine, A. (2000) The hypersensitive response facilitates plant infection by the necrotrophic pathogen *Botrytis cinerea*. *Curr Biol* **10**: 751–757.

Govrin, E.M., Rachmilevitch, S., Tiwari, B.S., Solomon, M., and Levine, A. (2006) An elicitor from *Botrytis cinerea* induces the hypersensitive response in *Arabidopsis thaliana* and other plants and promotes the Gray Mold disease. *Phytopathology* **96**: 299–307.

Hao, F., Ding, T., Wu, M., Zhang, J., Yang, L., Chen, W., and Li, G. (2018) Two novel hypovirulence-associated mycoviruses in the phytopathogenic fungus *Botrytis cinerea*: molecular characterization and suppression of infection cushion formation. *Viruses* **10**: 254.

Hou, J., Feng, H., Chang, H., Liu, Y., Li, G., Yang, S., *et al*. (2020) The H3K4 demethylase Jar1 orchestrates ROS production and expression of pathogenesis-related genes to facilitate *Botrytis cinerea* virulence. *New Phytol* **225**: 930–947.

Käll, L., Canterbury, J.D., Weston, J., Noble, W.S., and MacCoss, M.J. (2007) Semi-supervised learning for peptide identification from shotgun proteomics datasets. *Nat Methods* **4**: 923–925.

Kars, I., Krooshof, G.H., Wagemakers, L., Joosten, R., Benen, J.A.E., and Kan, J.A.L.V. (2005) Necrotizing activity of five *Botrytis cinerea* endopolygalacturonases produced in *Pichia pastoris*. *Plant J* **43**: 213–225.

Kelloniemi, J., Trouvelot, S., Héloir, M.-C., Simon, A., Dalmais, B., Frettinger, P., *et al*. (2015) Analysis of the molecular dialogue between Gray Mold (*Botrytis cinerea*) and grapevine (*Vitis vinifera*) reveals a clear shift in defense mechanisms during berry ripening. *Mol Plant Microbe Interact* **28**: 1167–1180.

Kong, W., Chen, N., Liu, T., Zhu, J., Wang, J., He, X., and Jin, Y. (2015) Large-scale transcriptome analysis of cucumber and *Botrytis cinerea* during infection. *PLoS One* **10**: e0142221.

Kuroki, M., Okauchi, K., Yoshida, S., Ohno, Y., Murata, S., Nakajima, Y., *et al*. (2017) Chitin-deacetylase activity induces appressorium differentiation in the rice blast fungus *Magnaporthe oryzae*. *Sci Rep* **7**: 9697.

Lam, W.C., Upadhya, R., Specht, C.A., Ragsdale, A.E., Hole, C.R., Levitz, S.M., and Lodge, J.K. (2019) Chitosan biosynthesis and virulence in the human fungal pathogen *Cryptococcus gattii*. *mSphere* **4**: e00644-19.

Li, Y., Han, Y., Qu, M., Chen, J., Chen, X., Geng, X., *et al*. (2020) Apoplastic cell death-inducing proteins of filamentous plant pathogens: roles in plant-pathogen interactions. *Front Genet* **11**: 661.

Liu, J.-K., Chang, H.-W., Liu, Y., Qin, Y.H., Ding, Y.-H., Wang, L., *et al*. (2018) The key gluconeogenic gene *PCK1* is crucial for virulence of *Botrytis cinerea* via initiating its conidial germination and host penetration: gluconeogenesis regulates *B*. *cinerea* pathogenesis. *Environ Microbiol* **20**: 1794–1814.

Liu, T., Chen, G., Min, H., and Lin, F. (2009) MoFLP1, encoding a novel fungal fasciclin-like protein, is involved in conidiation and pathogenicity in *Magnaporthe oryzae*. *J Zhejiang Univ Sci B* **10**: 434–444.

Liu, Z., Gay, L.M., Tuveng, T.R., Agger, J.W., Westereng, B., Mathiesen, G., *et al*. (2017) Structure and function of a broad-specificity chitin deacetylase from *Aspergillus nidulans* FGSC A4. *Sci Rep* **7**: 1746.

Livak, K.J., and Schmittgen, T.D. (2001) Analysis of relative gene expression data using real-time quantitative PCR and the $2^{-\Delta\Delta CT}$ method. *Methods* **25**: 402–408.

Lombard, V., Golaconda Ramulu, H., Drula, E., Coutinho, P. M., and Henrissat, B. (2014) The carbohydrate-active enzymes database (CAZy) in 2013. *Nucleic Acids Res* **42**: D490–D495.

Lumsden, R.D., and Wergin, W.P. (1980) Scanning-electron microscopy of infection of bean by species of *Sclerotinia*. *Mycologia* **72**: 1200–1209.

Mani, I., Sharma, V., Tamboli, I., and Raman, G. (2001) Interaction of melanin with proteins – the importance of an acidic intramelanosomal pH. *Pigment Cell Res* **14**: 170–179.

Marschall, R., and Tudzynski, P. (2016a) BcIqg1, a fungal IQGAP homolog, interacts with NADPH oxidase, MAP kinase and calcium signaling proteins and regulates virulence and development in *Botrytis cinerea*: BcIqg1-a central scaffold protein in *Botrytis cinerea*. *Mol Microbiol* **101**: 281–298.

Marschall, R., and Tudzynski, P. (2016b) Reactive oxygen species in development and infection processes. *Semin Cell Dev Biol* **57**: 138–146.

Marschall, R., and Tudzynski, P. (2017) The protein disulfide Isomerase of *Botrytis cinerea*: an ER protein involved in protein folding and redox homeostasis influences NADPH oxidase signaling processes. *Front Microbiol* **8**: 960.

Massaroli, M., Moraga, J., Bastos Borges, K., Ramírez-Fernández, J., Viaud, M., González Collado, I., *et al*. (2013) A shared biosynthetic pathway for botcinins and botrylactones revealed through gene deletions. *ChemBioChem* **14**: 132–136.

Mentges, M., Glasenapp, A., Boenisch, M., Malz, S., Henrissat, B., Frandsen, R.J.N., *et al*. (2020) Infection cushions of *Fusarium graminearum* are fungal arsenals for wheat infection. *Mol Plant Pathol* **21**: 1-18.

Michielse, C.B., Becker, M., Heller, J., Moraga, J., Collado, I. G., and Tudzynski, P. (2011) The *Botrytis cinerea* Reg1 protein, a putative transcriptional regulator, is required for pathogenicity, conidiogenesis, and the production of secondary metabolites. *Mol Plant Microbe Interact* **24**: 1074–1085.

Mitchell, A.L., Attwood, T.K., Babbitt, P.C., Blum, M., Bork, P., Bridge, A., *et al*. (2018) InterPro in 2019: improving coverage, classification and access to protein sequence annotations. *Nucleic Acids Res* **47**: D351–D360.

Nafisi, M., Stranne, M., Zhang, L., van Kan, J.A.L., and Sakuragi, Y. (2014) The endo-arabinanase BcAra1 is a novel host-specific virulence factor of the necrotic fungal phytopathogen *Botrytis cinerea*. *Mol Plant Microbe Interact* **27**: 781–792.

Nie, J., Yin, Z., Li, Z., Wu, Y., and Huang, L. (2019) A small cysteine-rich protein from two kingdoms of microbes is recognized as a novel pathogen-associated molecular pattern. *New Phytol* **222**: 995–1011.

Noda, J., Brito, N., and González, C. (2010) The *Botrytis cinerea* xylanase Xyn11A contributes to virulence with its necrotizing activity, not with its catalytic activity. *BMC Plant Biol* **10**: 38.

O'Connell, R., Thon, M., Hacquard, S., Amyotte, S.G., Kleemann, J., Torres, M.F., *et al*. (2012) Lifestyle transitions in plant pathogenic *Colletotrichum* fungi deciphered by genome and transcriptome analyses. *Nat Genet* **44**: 1060–1065.

Patel, P.K., and Free, S.J. (2019) The genetics and biochemistry of cell wall structure and synthesis in *Neurospora crassa*, a model filamentous fungus. *Front Microbiol* **10**: 2294.

Pepin, R. (1980) Le comportement parasitaire de *Sclerotinia tuberosa (hedw.) Fuckel* sur *Anemone nemorosa L*. Etude en microscopie photonique et électronique a balayage. *Mycopathologia* **72**: 89–99.

Perez-Dulzaides, R., Camacho, E., Cordero, R.J.B., and Casadevall, A. (2018) Cell-wall dyes interfere with *Cryptococcus neoformans* melanin deposition. *Microbiology* **164**: 1012–1022.

Pérez-Hernández, A., González, M., González, C., van Kan, J. A.L., and Brito, N. (2017) BcSUN1, a *B*. *cinerea* SUN-family protein, is involved in virulence. *Front Microbiol* **8**: 35.

Perez-Riverol, Y., Csordas, A., Bai, J., Bernal-Llinares, M., Hewapathirana, S., Kundu, D.J., *et al*. (2019) The PRIDE database and related tools and resources in 2019: improving support for quantification data. *Nucleic Acids Res* **47**: D442–D450.

Pineda, E., Thonnus, M., Mazet, M., Mourier, A., Cahoreau, E., Kulyk, H., *et al*. (2018) Glycerol supports growth of the *Trypanosoma brucei* bloodstream forms in the absence of glucose: analysis of metabolic adaptations on glycerol-rich conditions. *PLoS Pathog* **14**: e1007412.

Pinedo, C., Moraga, J., Barua, J., González-Rodríguez, V. E., Aleu, J., Durán-Patrón, R., *et al*. (2016) Chemically induced cryptic sesquiterpenoids and expression of sesquiterpene cyclases in *Botrytis cinerea* revealed new

sporogenic (+)-4- *Epi* eremophil-9-en-11-ols. *ACS Chem Biol* **11**: 1391–1400.

Porquier, A., Moraga, J., Morgant, G., Dalmais, B., Simon, A., Sghyer, H., *et al*. (2019) Botcinic acid biosynthesis in *Botrytis cinerea* relies on a subtelomeric gene cluster surrounded by relics of transposons and is regulated by the Zn2Cys6 transcription factor BcBoa13. *Curr Genet* **65**: 965–980.

Priebe, S., Kreisel, C., Horn, F., Guthke, R., and Linde, J. (2015) FungiFun2: a comprehensive online resource for systematic analysis of gene lists from fungal species. *Bioinformatics* **31**: 445–446.

Prior, G., and Owen, J. (1964) Pathological anatomy of *Sclerotinia trifoliorum* on clover and alfalfa. *Phytopathology* **54**: 784–787.

Qutob, D., Kemmerling, B., Brunner, F., Küfner, I., Engelhardt, S., Gust, A.A., *et al*. (2006) Phytotoxicity and innate immune responses induced by Nep1-like proteins. *Plant Cell* **18**: 3721–3744.

R Core Team. (2019) *R: A Language and Environment for Statistical Computing*. Vienna, Austria: R Foundation for Statistical Computing. https://www.R-project.org/.

Rascle, C., Dieryckx, C., Dupuy, J.W., Muszkieta, L., Souibgui, E., Droux, M., *et al*. (2018) The pH regulator PacC: a host-dependent virulence factor in *Botrytis cinerea*. *Environ Microbiol Rep* **10**: 555–568.

Rheinländer, P.A., Sutherland, P.W., and Fullerton, R.A. (2013) Fruit infection and disease cycle of *Botrytis cinerea* causing cosmetic scarring in persimmon fruit (*Diospyros kaki* Linn.). *Aust Plant Pathol* **42**: 551–560.

Rolke, Y., Liu, S., Quidde, T., Williamson, B., Schouten, A., Weltring, K.-M., *et al*. (2004) Functional analysis of $H_2O_2$-generating systems in *Botrytis cinerea*: the major Cu-Zn-superoxide dismutase (BCSOD1) contributes to virulence on French bean, whereas a glucose oxidase (BCGOD1) is dispensable. *Mol Plant Pathol* **5**: 17–27.

Rossi, F.R., Gárriz, A., Marina, M., Romero, F.M., Gonzalez, M.E., Collado, I.G., and Pieckenstain, F.L. (2011) The sesquiterpene botrydial produced by *Botrytis cinerea* induces the hypersensitive response on plant tissues and its action is modulated by salicylic acid and jasmonic acid signaling. *Mol Plant Microbe Interact* **24**: 888–896.

Ryder, L.S., and Talbot, N.J. (2015) Regulation of appressorium development in pathogenic fungi. *Curr Opin Plant Biol* **26**: 8–13.

Sapmak, A., Boyce, K.J., Andrianopoulos, A., and Vanittanakom, N. (2015) The pbrB gene encodes a laccase required for DHN-melanin synthesis in conidia of *Talaromyces (Penicillium) marneffei*. *PLoS One* **10**: e0122728.

Schouten, A., Baarlen, P.V., and Kan, J.A.L.V. (2008) Phytotoxic Nep1-like proteins from the necrotrophic fungus *Botrytis cinerea* associate with membranes and the nucleus of plant cells. *New Phytol* **177**: 493–505.

Schumacher, J. (2016) DHN melanin biosynthesis in the plant pathogenic fungus *Botrytis cinerea* is based on two developmentally regulated key enzyme (PKS)-encoding genes: DHN melanogenesis in *Botrytis cinerea*. *Mol Microbiol* **99**: 729–748.

Segmüller, N., Kokkelink, L., Giesbert, S., Odinius, D., van Kan, J., and Tudzynski, P. (2008) NADPH oxidases are involved in differentiation and pathogenicity in *Botrytis cinerea*. *MPMI* **21**: 808–819.

Seifert, G. (2018) Fascinating fasciclins: a surprisingly widespread family of proteins that mediate interactions between the cell exterior and the cell surface. *Int J Mol Sci* **19**: 1628.

Sharman, S., and Heale, J.B. (1977) Penetration of carrot roots by the grey mould fungus *Botrytis cinerea* Pers. ex Pers. *Physiol Plant Pathol* **10**: 63–71.

Shlezinger, N., Minz, A., Gur, Y., Hatam, I., Dagdas, Y.F., Talbot, N.J., and Sharon, A. (2011) Anti-apoptotic machinery protects the necrotrophic fungus *Botrytis cinerea* from host-induced apoptotic-like cell death during plant infection. *PLoS Pathog* **7**: e1002185.

Siegmund, U., and Viefhues, A. (2016) Reactive oxygen species in the *Botrytis* – host interaction. In *Botrytis – The fungus, the pathogen and its management in agricultural systems*, Fillinger, S., and Elad, Y. (eds). Cham: Springer International Publishing, pp. 269–289.

Simon, A., and Biot, E. (2010) ANAIS: analysis of NimbleGen arrays interface. *Bioinformatics* **26**: 2468–2469.

Simon, A. and Viaud, M. (2018) *Cross-reference table for Botrytis cinerea B0510 and T4 gene ids*. URL https://doi.org/10.15454/IHYJCX, Portail Data INRAE, V2, UNF:6:PgcjbcKsoyoUHnNO6LX9Vg== [fileUNF]

Smith, V., Punja, Z., and Jenkins, S. (1986) A histological study of infection of host tissue by *Sclerotium rolfsii*. *Phytopathology* **76**: 755–759.

Soanes, D.M., Chakrabarti, A., Paszkiewicz, K.H., Dawe, A. L., and Talbot, N.J. (2012) Genome-wide transcriptional profiling of appressorium development by the rice blast fungus *Magnaporthe oryzae*. *PLoS Pathog* **8**: e1002514.

Stewart, A., Backhouse, D., Sutherland, P.W., and Fullerton, R.A. (1989) The development of infection structures of *Sclerotium cepivorum* on onion. *J Phytopathol* **126**: 22–32.

Sun, L.-L., Li, M., Suo, F., Liu, X.-M., Shen, E.-Z., Yang, B., *et al*. (2013) Global analysis of fission yeast mating genes reveals new autophagy factors. *PLoS Genet* **9**: e1003715.

Tariq, V.N., and Jeffries, P. (1984) Appressorium formation by *Sclerotinia sclerotiorum*: scanning electron microscopy. *Trans Br Mycol Soc* **82**: 645–651.

Ten Have, A., Espino, J.J., Dekkers, E., Van Sluyter, S.C., Brito, N., Kay, J., *et al*. (2010) The *Botrytis cinerea* aspartic proteinase family. *Fungal Genet Biol* **47**: 53–65.

Upadhya, R., Baker, L.G., Lam, W.C., Specht, C.A., Donlin, M.J., and Lodge, J.K. (2018) *Cryptococcus neoformans* Cda1 and Its Chitin Deacetylase Activity Are Required for Fungal Pathogenesis. *mBio* **9**: e02087-18.

Van den Brink, J., and de Vries, R.P. (2011) Fungal enzyme sets for plant polysaccharide degradation. *Appl Microbiol Biotechnol* **91**: 1477–1492.

Van den Heuvel, J., and Waterreus, L.P. (1983) Conidial concentration as an important factor determining the type of prepenetration structures formed by *Botrytis cinerea* on leaves of French bean (*Phaseolus vulgaris*). *Plant Pathol* **32**: 263–272.

Van Kan, J.A.L., Stassen, J.H.M., Mosbach, A., Van Der Lee, T. A.J., Faino, L., Farmer, A.D., *et al*. (2017) A gapless genome sequence of the fungus *Botrytis cinerea*: gapless genome sequence of *B. cinerea*. *Mol Plant Pathol* **18**: 75–89.

Viefhues, A., Heller, J., Temme, N., and Tudzynski, P. (2014) Redox systems in *Botrytis cinerea*: impact on development and virulence. *Mol Plant Microbe Interact* **27**: 858–874.

Viefhues, A., Schlathoelter, I., Simon, A., Viaud, M., and Tudzynski, P. (2015) Unraveling the function of the response regulator BcSkn7 in the stress signaling network of *Botrytis cinerea*. *Eukaryot Cell* **14**: 636–651.

Vu, V.V., Beeson, W.T., Span, E.A., Farquhar, E.R., and Marletta, M.A. (2014) A family of starch-active polysaccharide monooxygenases. *Proc Natl Acad Sci U S A* **111**: 13822–13827.

Xie, M., Zhao, X., Lü, Y., and Jin, C. (2020) Chitin deacetylases Cod4 and Cod7 are involved in polar growth of *Aspergillus fumigatus*. *Microbiology* **9**: e00943.

Yu, J.-H., Hamari, Z., Han, K.-H., Seo, J.-A., Reyes-Domínguez, Y., and Scazzocchio, C. (2004) Double-joint PCR: a PCR-based molecular tool for gene manipulations in filamentous fungi. *Fungal Genet Biol* **41**: 973–981.

Zhang, L., De Wu, M., Li, G.Q., Jiang, D.H., and Huang, H. C. (2010) Effect of Mitovirus infection on formation of infection cushions and virulence of *Botrytis cinerea*. *Physiol Mol Plant Pathol* **75**: 71–80.

Zhang, M.-Z., Sun, C.-H., Liu, Y., Feng, H.-Q., Chang, H.-W., Cao, S.-N., *et al*. (2020) Transcriptome analysis and functional validation reveal a novel gene, BcCGF1, that enhances fungal virulence by promoting infection-related development and host penetration. *Mol Plant Pathol* **21**: 834–853.

Zhang, W., Corwin, J.A., Copeland, D.H., Feusier, J., Eshbaugh, R., Cook, D.E., *et al*. (2019) Plant–necrotroph co-transcriptome networks illuminate a metabolic battlefield. *Elife* **8**: e44279.

Zhang, Y., Zhang, Y., Qiu, D., Zeng, H., Guo, L., and Yang, X. (2015) BcGs1, a glycoprotein from *Botrytis cinerea*, elicits defence response and improves disease resistance in host plants. *Biochem Biophys Res Commun* **457**: 627–634.

Zhu, W., Ronen, M., Gur, Y., Minz-Dub, A., Masrati, G., Ben-Tal, N., *et al*. (2017) BcXYG1, a secreted Xyloglucanase from *Botrytis cinerea*, triggers both cell death and plant immune responses. *Plant Physiol* **175**: 438–456.

## Supporting Information

Additional Supporting Information may be found in the online version of this article at the publisher's web-site:

**Appendix S1**: Supporting Information

**Table S1.** Microarray analysis of the infection cushion of Botrytis cinerea.

**Table S2.** RT-qPCR validation of microarray expression profiles from the infection cushion of Botrytis cinerea produced in vitro.

**Table S3.** Up-accumulated proteins in the secretome of the infection cushion of Botrytis cinerea.

**Table S4.** Constructs and primers used in this study.